Measurement 204 (2022) 112047

Contents lists available at ScienceDirect

Measurement

journal homepage: www.elsevier.com/locate/measurement

Analysis of DOV estimation in initial alignment based on Single-axis rotating SINS

Shiwen Hao, Zhili Zhang *, Zhaofa Zhou, Zhenjun Chang, Zhihao Xu, Xinyu Li

Xi'an Research Institute of High-Tech, 710025, China

ARTICLE INFO

Keywords:
Deflection of the vertical
Strapdown inertial navigation system
Initial alignment
Rotating modulation
Misalignment angles
Kalman filter

ABSTRACT

The Strapdown inertial navigation system (SINS) requires the precise attitude, whereas the deflection of the vertical (DOV) is normally ignored in alignment. To solve the issue of orientation and position errors caused by DOV, a novel DOV calculation method, estimated by misalignment angles based on single-axis rotating modulation, is proposed. The theoretical limit error equation of attitude angle, affected by the coupling of inertial measurement units (IMU) errors and DOV, has been specifically derived based on the inertial frame alignment theory. It is pointed out that the DOV components directly affect the values of misalignment angles, coupling with horizontal accelerometer errors. Moreover, the specific process of combining coarse alignment of inertial frame and fine alignment of Kalman filter method is presented. Finally, the experiment analysis validates the performance of the proposed method and correctness of the theoretical analysis, where the estimation accuracies of DOV components are 0.349″ and 0.479″ respectively.

1. Introduction

HE initial alignment is the first and significant step for strapdown inertial navigation system (SINS) to achieve high-precision position and orientation, which is mainly obtaining the initial coordinate transformation matrix from the body frame (b) to the navigation frame (n, ellipsoid normal plane) as the initial condition for the following navigation calculation [1–4]. For the traditional SINS navigation process, due to the limitation for the precision of inertial measurement units, the plump line on the geoid and the normal line on the ellipsoid are considered as the same ignoring the influence of DOV. However, with the development of inertial technology and requirements of high-precision navigation in recent decades, the DOV has become one of the main error sources in initial alignment and navigation [5–7].

As the irregular surface and uneven internal density of the Earth, the ellipsoid, resembling the geoid, was put forward to briefly describe the gravity field of the Earth in navigation and orientation [8–10]. The difference between the two definitions (geoid and ellipsoid) derivate the definitions of gravity disturbance vector (GDV) and DOV, which were specifically introduced in chapterIII. Hence, the analysis of error influence and the effective measurement of GDV and DOV in SINS have become the top issue in improving the precision of navigation and orientation. In this respect, Hanson et.al [11] investigated the correlation between the DOV and uncalibrated zero biases of accelerometers in initial alignment. Jekeli et.al [12] analyzed the precision improvement of inertial navigation system (INS) after GDV compensation. Unfortunately, the corresponding conclusions were qualitative and not universal. Fang et.al [13] investigated the gravity compensation method for airborne position and orientation system. Chang et.al [14] investigated the GDV compensation for INS and analyzed the performances of INS in different compensation cases. In addition, Kwon et.al [15] investigated the requirements for gravity compensation in Ultra-precise INS. Zhu et. al [16] proposed a real-time gravity compensation method for attitude calculation based on Kalman filter and constructed a Markov model based on the gravity map. Due to the precision improvement of gravity field spherical harmonic models (SHM), utilizing the SHM to conduct DOV compensation for initial alignment and navigation has also become another topic. Wang et.al [17] discussed the accuracy of truncated SHM for application in INS. Tie et.al [18] investigated the effect of horizontal gravity disturbance compensation for high-precision INS. Wu et.al [19] investigated the gravity compensation effect using EGM2008 for long-term INS.

From the perspective of DOV calculations, the astrogeodetic, gravimetric, levelling measurement and Global Satellite System (GNSS) based

* Corresponding author.
E-mail addresses: wenjy70796@163.com (S. Hao), aaa360070796@qq.com (Z. Zhang), zzftxy@163.com (Z. Zhou), changzj2105@163.com (Z. Chang), xuzh_aca@163.com (Z. Xu), 1025997454@qq.com (X. Li).

https://doi.org/10.1016/j.measurement.2022.112047
Received 27 March 2022; Received in revised form 4 October 2022; Accepted 7 October 2022
Available online 7 November 2022

satellite methods are the most common means for DOV determination in recent decades. Utilizing the astronomic and geodetic latitudes and longitudes of the same point is the principle of astrogeodetic methods, where the most classical representative is observing the astronomic coordinates by digital zenith camera system [20]. However, restriction by weather and inefficient measurement restraint this method's application. In recent years, the DOV calculation based on SINS/GNSS, which adopting the attitude difference patten, has been developed a mainstream. Dai et.al [21] constructed the model of attitude reference error and inertial sensors errors. Zhu et.al [22] investigated the attitude difference method to estimate DOV in real time. Hao et.al [23] analyzed the attitude error caused by DOV in INS/GNSS base. An et.al [24] investigated the estimation of attitude angles based on fading memory Kalman filter after DOV compensation. However, most efforts of the previous work are almost either devoted to constructing the attitude reference model based on GNSS or directly compensating the DOV in INS without specific error analysis of DOV based on the theory of initial alignment. With this consideration, this paper specifically derived the error influence principle of DOV in inertial frame alignment and proposed the DOV calculation method by misalignment angular observation based on single-axis rotation.

The contents are organized as follows: the reference coordinate frames are briefly defined in Section II; Section III describes the definitions of the gravity field and theory of inertial frame alignment; the error equations of SINS and error analysis of DOV based on inertial frame alignment are specifically described in Section IV; in Section V, the DOV calculation process based on single-axis rotation is introduced and the Kalman filter model is constructed; the experiments are conducted in Section VI; eventually, conclusion are presented in Section VII.

2. Reference frame definitions

In the inertial space, there are six degrees of freedom during the carrier movement including three angles and linear movements respectively. Consequently, the carrier motion can be precisely described by angular and linear movements in three directions. For the strapdown inertial navigation system, the navigation calculation will inevitably involve several reference frame definitions, and the attitude calculation is based on vector transformation between the different frames. Therefore, the several frames involved in this paper are illustrated in this section.

1) Inertial coordinate frame (i frame, $O_iX_iY_iZ_i$).

Generally, the center of the reference ellipsoid model is selected as the coordinate origin, the O_iZ_i axis points to the north pole along the direction of the earth's axis, and the O_iX_i and O_iY_i axes located in the earth's equatorial plane. The *i* frame is static with respect to the distant galaxies.

2) Geographic coordinate frame (g frame, $O_gX_gY_gZ_g$).

It is defined that the origin of the coordinates is located at the center of mass of the carrier, the O_gX_g axis and the O_gY_g axis located in the local horizontal plane, and point to the east and north directions respectively, and the ellipsoid normal direction of the O_gZ_g axis points to the up that is, "E-*N*-U".

3) Navigation coordinate frame (n frame, $O_nX_nY_nZ_n$).

The navigation coordinate frame is defined as a unified frame used for navigation calculations. The g frame is selected as the n frame in this paper.

4) Body coordinate frame (b frame, $O_bX_bY_bZ_b$).

The mass center is defined as the origin of the b frame, and the O_bX_b, O_bY_b, and O_bZ_b point to the right, front, and up of the carrier, respectively.

5) Strapdown platform coordinate frame (n' frame).

Strapdown platform coordinate frame is defined as the navigation frame calculated by SINS, which has a small deviation from the real navigation coordinate frame (n).

6) Body inertial coordinate frame (ib_0 frame).

It is defined the initial moment of the (b) frame in alignment. The ib_0 frame is stable relative to the inertial space.

7) Navigation inertial coordinate frame (in_0 frame).

The initial moment of the (n) frame in alignment is defined as the navigation inertial coordinate frame. The ib0 frame is also stable relative to the inertial space.

8) Inertial measurement units (IMU) coordinate frame (s).

The origin of the coordinate is located at the origin of the accelerometer unit, and the three axes point in the direction of the nominal sensitive axis of the inertial sensors. While the IMU is no rotation relative to b frame, the s frame is consistent with b frame.

3. Gravity field and initial alignment

3.1. Definition of the gravity field

The geoid was proposed in 1873, which is the gravity equipotential surface of the earth. Due to the geoid cannot be described by a mathematical model, the reference ellipsoid was put forward to approximate the geoid. Consequently, the gravimetric DOV is defined as the difference between the plump line in the geoid and the normal line in the reference ellipsoid, as shown in Fig. 1. The DOV components in the west-to-east direction and the south-to-north direction are η, ξ respectively. As shown in Fig. 2, the difference between the true gravity vector on the geoid and the normal gravity vector on the reference ellipsoid is called the Gravity Disturbance Vector (GDV), which can be expressed as:

$$\delta g^n = [\,-\eta g_0 \quad -\xi g_0 \quad \Delta g\,]^T \tag{1}$$

where g_0 denotes the normal gravity value of a point, which can be

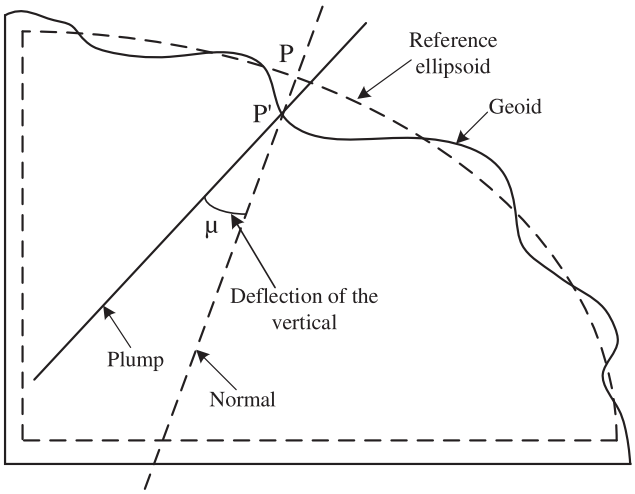

Fig. 1. Gravimetric deflection of the vertical.

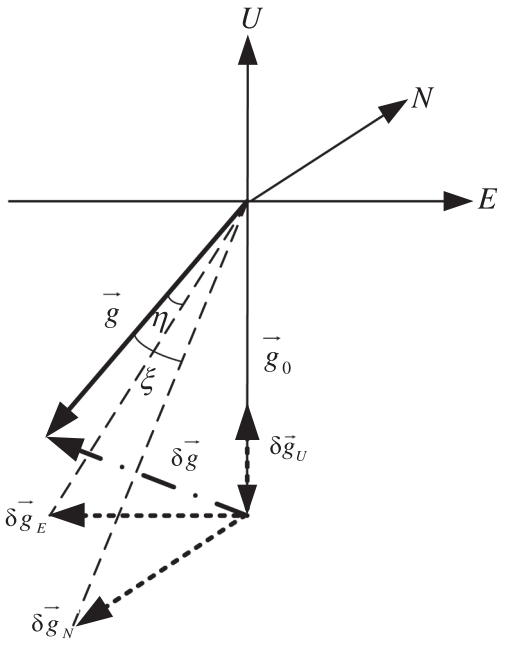

Fig. 2. Gravity disturbance vector.

calculated by formula (2), Δg is defined as gravity anomaly that reflects the value deviation of the two gravity definitions, which can be expressed as formula (3).

$$g_0 = 9.780327 \times \begin{pmatrix} 1 + 0.00527094 \times \sin^2 L \\ +0.0000232718 \times \sin^2 2L \end{pmatrix} - 0.3086 \times 10^{-5} h \tag{2}$$

$$\Delta g = g - g_0 \tag{3}$$

In terms of geodetic coordinate, L and B mean the geodetic latitude and longitude of a point, respectively, while in the astronomic coordinate, φ and λ reflect the astronomic latitude and longitude of the same point, respectively.

3.2. Inertial frame alignment

Initial alignment, calculation of attitude transformation matrix$\boldsymbol{C}_{\mathrm{b}}^{\mathrm{n}}$, is the process that determines the initial attitude of SINS. Inertial frame alignment is one of the most classical vector calculation methods, where the matrix $\boldsymbol{C}_{\mathrm{b}}^{\mathrm{n}}$ can be divided into the form of multiplying three matrices. The attitude matrix can be expressed as follows according to the characters.

$$C_b^n = C_{i_{n0}}^n C_{i_{b0}}^{i_{n0}} C_b^{i_{b0}} \tag{4}$$

where $\boldsymbol{C}_{\mathrm{i_{n0}}}^{\mathrm{n}}$ represents the rotation of the (n) frame relative to the ($\mathrm{i_{no}}$) frame, which can be calculated by the latitude of the carrier location (L) and time (t), shown as:

$$\boldsymbol{C}_{\mathrm{i_{n0}}}^{\mathrm{n}} = \begin{bmatrix} -\sin[\omega_{\mathrm{ie}}(t-t_0)] & \cos[\omega_{\mathrm{ie}}(t-t_0)] & 0 \\ -\sin L\cos[\omega_{\mathrm{ie}}(t-t_0)] & -\sin L\sin[\omega_{\mathrm{ie}}(t-t_0)] & \cos L \\ \cos L\cos[\omega_{\mathrm{ie}}(t-t_0)] & \cos L\sin[\omega_{\mathrm{ie}}(t-t_0)] & \sin L \end{bmatrix} \tag{5}$$

where L is the latitude, ω_{ie} is the Earth's rotation rate.

In equation (4), $\boldsymbol{C}_{\mathrm{b}}^{\mathrm{i_{b0}}}$ represents the rotation of the body frame relative to the body inertial coordinate frame; its initial form is unity matrix$\boldsymbol{C}_{\mathrm{b}}^{\mathrm{i_{b0}}}(t_0) = \boldsymbol{I}$, The matrix $\boldsymbol{C}_{\mathrm{b}}^{\mathrm{i_{b0}}}(t)$ can be real-time updated from the gyroscope's angle increment using the quaternion method based on differential equation (6).

$$\dot{C}_b^{i_{b0}}(t) = C_b^{i_{b0}}(t)\left(\omega_{i_{b0}}^b \times\right) \tag{6}$$

Therefore, the key to calculate the matrix $\boldsymbol{C}_{\mathrm{b}}^{\mathrm{n}}$ is solving the matrix$\boldsymbol{C}_{\mathrm{i_{b0}}}^{\mathrm{i_{n0}}}$. In this algorithm, the gravity vectors$\boldsymbol{g}^{\mathrm{i_{b0}}}(t_1)$,$\boldsymbol{g}^{\mathrm{i_{b0}}}(t_2)$,$\boldsymbol{g}^{\mathrm{i_{n0}}}(t_1)$, and $\boldsymbol{g}^{\mathrm{i_{n0}}}(t_2)$ at two different moments in the $\mathrm{i_{b0}}$ and $\mathrm{i_{n0}}$ coordinate frames are selected as reference vectors to calculate$\boldsymbol{C}_{\mathrm{i_{b0}}}^{\mathrm{i_{n0}}}$, shown as equation (7).

$$\boldsymbol{C}_{\mathrm{i_{b0}}}^{\mathrm{i_{n0}}} = \begin{bmatrix} \left[\boldsymbol{g}^{\mathrm{i_{n0}}}(t_1)\right]^{\mathrm{T}} \\ \left[\boldsymbol{g}^{\mathrm{i_{n0}}}(t_1) \times \boldsymbol{g}^{\mathrm{i_{n0}}}(t_2)\right]^{\mathrm{T}} \\ \left[\boldsymbol{g}^{\mathrm{i_{n0}}}(t_1) \times \boldsymbol{g}^{\mathrm{i_{n0}}}(t_2) \times \boldsymbol{g}^{\mathrm{i_{n0}}}(t_1)\right]^{\mathrm{T}} \end{bmatrix}^{-1} \begin{bmatrix} \left[\boldsymbol{g}^{\mathrm{i_{b0}}}(t_1)\right]^{\mathrm{T}} \\ \left[\boldsymbol{g}^{\mathrm{i_{b0}}}(t_1) \times \boldsymbol{g}^{\mathrm{i_{b0}}}(t_2)\right]^{\mathrm{T}} \\ \left[\boldsymbol{g}^{\mathrm{i_{b0}}}(t_1) \times \boldsymbol{g}^{\mathrm{i_{b0}}}(t_2) \times \boldsymbol{g}^{\mathrm{i_{b0}}}(t_1)\right]^{\mathrm{T}} \end{bmatrix} \tag{7}$$

By substituting the obtained matrixes$\boldsymbol{C}_{\mathrm{b}}^{\mathrm{i_{b0}}}$,$\boldsymbol{C}_{\mathrm{i_{b0}}}^{\mathrm{i_{n0}}}$,$\boldsymbol{C}_{\mathrm{i_{n0}}}^{\mathrm{n}}$ into equation (4) correspondingly, the attitude transformation matrix can be obtained. When projecting accelerometer measurements to the $\mathrm{i_{b0}}$ frame, the attitude change of the carrier caused by carrier disturbance can be tracked, which can effectively suppress the waggling disturbance of the carrier.

4. Error analysis of inertial frame alignment

4.1. Inertial navigation error equation considering DOV

The mechanical arrangement of SINS is based on the specific force equation, shown as:

$$\dot{\boldsymbol{V}}^{\mathrm{n}} = \boldsymbol{C}_{\mathrm{b}}^{\mathrm{n}}\boldsymbol{f}^{\mathrm{b}} - \left(2\boldsymbol{\omega}_{\mathrm{ie}}^{\mathrm{n}} + \boldsymbol{\omega}_{\mathrm{en}}^{\mathrm{n}}\right) \times \boldsymbol{V}^{\mathrm{n}} + \boldsymbol{g}^{\mathrm{n}} \tag{8}$$

where $\boldsymbol{V}^{\mathrm{n}}$ denotes the velocity of carrier in navigation frame, $\boldsymbol{f}^{\mathrm{b}}$ means the specific force measured by accelerometer. $\boldsymbol{g}^{\mathrm{n}}$ means the projection of true gravity vector in navigation frame. $\boldsymbol{\omega}_{\mathrm{en}}^{\mathrm{n}}$ denotes the angle rate between the e frame and n frame.

Differentiate both sides of the above formula, the velocity error equation can be obtained as:

$$\begin{aligned} \delta\dot{V}^n = &(-\phi^n \times) f^n + C_b^n \nabla^b - \left(2\delta\omega_{ie}^n + \delta\omega_{en}^n\right) \times V^n \\ &- \left(2\omega_{ie}^n + \omega_{en}^n\right) \times \delta V^n + \delta g^n \end{aligned} \tag{9}$$

where $\delta\mathbf{V}^{\mathrm{n}}$ means the velocity error, $(\phi^{\mathrm{n}}\times)$ means the antisymmetric matrix of misalignment angle, ∇^{b} denotes the constant zero bias errors of accelerometers. $\delta\mathbf{g}^{\mathrm{n}}$ means the gravity disturbance error, shown as formula (1).

For the strapdown inertial navigation system, the attitude update follows with the attitude differential equation, shown as formula (10), while the attitude error equation can be obtained as formula (11).

$$\dot{\boldsymbol{C}}_{\mathrm{b}}^{\mathrm{n}} = \boldsymbol{C}_{\mathrm{b}}^{\mathrm{n}}(\boldsymbol{\omega}_{\mathrm{nb}}^{\mathrm{b}}\times) = \boldsymbol{C}_{\mathrm{b}}^{\mathrm{n}}(\boldsymbol{\omega}_{\mathrm{ib}}^{\mathrm{b}}\times) - \left(\boldsymbol{\omega}_{\mathrm{in}}^{\mathrm{n}} \times\right)\boldsymbol{C}_{\mathrm{b}}^{\mathrm{n}} \tag{10}$$

$$\dot{\phi}^n = -\omega_{in}^n \times \phi^n - C_b^n \varepsilon^b + \delta\omega_{in}^n \tag{11}$$

where $\begin{matrix} \delta\omega_{in}^n = \delta\omega_{ie}^n + \delta\omega_{en}^n \\ = M_1\delta V^n + M_2\delta p \end{matrix}$, $M_1 = \begin{bmatrix} 0 & -\frac{1}{R_M+h} & 0 \\ \frac{1}{R_N+h} & 0 & 0 \\ \frac{\tan L}{R_N+h} & 0 & 0 \end{bmatrix} M_2 = \begin{bmatrix} 0 & 0 & \frac{V_N}{(R_M+h)^2} \\ -\omega_{ie}\sin L & 0 & -\frac{V_E}{(R_N+h)^2} \\ \omega_{ie}\cos L + \frac{V_E\sec^2 L}{R_N+h} & 0 & \frac{-V_E\tan L}{(R_N+h)^2} \end{bmatrix}$, $\boldsymbol{\varepsilon}^{\mathrm{b}}$ means the constant drift bias errors of gyroscopes, $\boldsymbol{p}$ reflects the position information, i.e, latitude, longitude and elevation $\boldsymbol{p} = [L\ \lambda\ h]^{\mathrm{T}}$.

It is indicated from formula (9) and (11) that the DOV firstly influences velocity errors of carrier through the velocity channel, and then affect the attitude errors. Therefore, the DOV information should be

reflected in attitude errors of carrier. The error analysis of inertial frame alignment will be introduced in the next section.

4.2. Error analysis of inertial frame alignment

Under the ideal conditions, the attitude transformation matrix can be calculated by equation (4). However, due to the existence of IMU errors and the gravity field model error, the estimation of $\widehat{\boldsymbol{C}}_{\mathrm{b}}^{\mathrm{n}}$ should be calculated by the following formula:

$$\widehat{\boldsymbol{C}}_{\mathrm{b}}^{\mathrm{n}} = \widehat{\boldsymbol{C}}_{\mathrm{i_{n0}}}^{\mathrm{n}}\,\widehat{\boldsymbol{C}}_{\mathrm{i_{b0}}}^{\mathrm{i_{n0}}}\,\widehat{\boldsymbol{C}}_{\mathrm{b}}^{\mathrm{i_{b0}}} \tag{12}$$

where the matrixes$\widehat{\boldsymbol{C}}_{\mathrm{i_{n0}}}^{\mathrm{n}}$,$\widehat{\boldsymbol{C}}_{\mathrm{i_{b0}}}^{\mathrm{i_{n0}}}$, $\widehat{\boldsymbol{C}}_{\mathrm{b}}^{\mathrm{i_{b0}}}$ include the error items respectively.

Differentiate both sides of the above formula, the error equation is given by:

$$\delta C_b^n = \delta C_{i_{n0}}^n C_{i_{b0}}^{i_{n0}} C_b^{i_{b0}} + C_{i_{n0}}^n \delta C_{i_{b0}}^{i_{n0}} C_b^{i_{b0}} + C_{i_{n0}}^n C_{i_{b0}}^{i_{n0}} \delta C_b^{i_{b0}} \tag{13}$$

For the static-base alignment, due to the latitude of carrier and rotation angular rate of earth can be obtained precisely, the above formula can be simplified as:

$$\delta C_b^n = C_{i_{n0}}^n \delta C_{i_{b0}}^{i_{n0}} C_b^{i_{b0}} + C_{i_{n0}}^n C_{i_{b0}}^{i_{n0}} \delta C_b^{i_{b0}} \tag{14}$$

From the relation between the misalignment angle and attitude error matrix, the following formula can be obtained:

$$\delta C_b^n = -\phi^n \times C_b^n \tag{15}$$

$$\delta C_{i_{b0}}^{i_{n0}} = -\phi_1^{i_{n0}} \times C_{i_{b0}}^{i_{n0}} \tag{16}$$

$$\delta C_b^{i_{b0}} = -\phi_2^{i_{b0}} \times C_b^{i_{b0}} \tag{17}$$

Substitute the above equations into the formula (14), the formula can be rewritten as:

$$\begin{aligned} -\phi^n \times C_b^n &= -\phi^n \times C_{i_{b0}}^n C_b^{i_{b0}} \\ &= C_{i_{n0}}^n \left(-\phi^{i_{n0}} \times\right) C_{i_{b0}}^{i_{n0}} C_b^{i_{b0}} + C_{i_{n0}}^n C_{i_{b0}}^{i_{n0}} \left(-\phi^{i_{b0}} \times\right) C_b^{i_{b0}} \end{aligned} \tag{18}$$

Multiply the matrix $\boldsymbol{C}_{\mathrm{n}}^{\mathrm{i_{b0}}}$ to both sides of the above formula, according to the theory of matrix similar changes, the simplified equation can be obtained as:

$$\begin{aligned} -\phi^{\mathrm{n}}\times &= \boldsymbol{C}_{\mathrm{i_{n0}}}^{\mathrm{n}}\left(-\phi^{\mathrm{i_{n0}}}\times\right)\boldsymbol{C}_{\mathrm{n}}^{\mathrm{i_{n0}}} + \boldsymbol{C}_{\mathrm{i_{b0}}}^{\mathrm{n}}\left(-\phi^{\mathrm{i_{b0}}}\times\right)\boldsymbol{C}_{\mathrm{n}}^{\mathrm{i_{b0}}} \\ &= -\left(\boldsymbol{C}_{\mathrm{i_{n0}}}^{\mathrm{n}}\phi^{\mathrm{i_{n0}}}\times\right) - \left(\boldsymbol{C}_{\mathrm{i_{b0}}}^{\mathrm{n}}\phi^{\mathrm{i_{b0}}}\times\right) \end{aligned} \tag{19}$$

Consequently, the misalignment angle (ϕ^{n}) of attitude error matrix ($\delta\boldsymbol{C}_{\mathrm{b}}^{\mathrm{n}}$) can be divided into two components, the projections (ϕ_1^{n}) and (ϕ_2^{n}) in (n) frame of the misalignment angle ($\phi_1^{\mathrm{i_{n0}}}$) and ($\phi_2^{\mathrm{i_{b0}}}$) respectively, shown as formula (20).

$$\begin{aligned} \phi^{\mathrm{n}} &= \left(\boldsymbol{C}_{\mathrm{i_{n0}}}^{\mathrm{n}}\phi_1^{\mathrm{i_{n0}}}\right) + \left(\boldsymbol{C}_{\mathrm{i_{b0}}}^{\mathrm{n}}\phi_2^{\mathrm{i_{b0}}}\right) \\ &= \phi_1^{\mathrm{n}} + \phi_2^{\mathrm{n}} \end{aligned} \tag{20}$$

1) misalignment angle ϕ_2^{n} analysis.

For the measurement of SINS, the gravity vector projection under inertial body frame ($\mathrm{i_{b0}}$) is generally calculated by specific force measured by accelerometers ($\widetilde{\boldsymbol{f}}^{\mathrm{b}}(t)$), given by:

$$\widetilde{\boldsymbol{g}}^{\mathrm{i_{b0}}}(t) = -\widehat{\boldsymbol{C}}_{\mathrm{b}}^{\mathrm{i_{b0}}}(t)\widetilde{\boldsymbol{f}}^{\mathrm{b}}(t) \tag{21}$$

According to the equation (7) and (21), the error of matrix ($\widehat{\boldsymbol{C}}_{\mathrm{b}}^{\mathrm{i_{b0}}}(t)$) also have an impact on the matrix ($\widehat{\boldsymbol{C}}_{\mathrm{i_{b0}}}^{\mathrm{i_{n0}}}(t)$). Hence, the error of matrix ($\widehat{\boldsymbol{C}}_{\mathrm{b}}^{\mathrm{i_{b0}}}(t)$) is initially introduced in this section.

When the measurement error of the gyroscopes is not considering, the matrix ($\boldsymbol{C}_{\mathrm{b}}^{\mathrm{i_{b0}}}$) follows with the equation (22), while on the contrary, the differential equation of matrix ($\widehat{\boldsymbol{C}}_{\mathrm{b}}^{\mathrm{i_{b0}}}$) is given as equation (23).

$$\dot{\boldsymbol{C}}_{\mathrm{b}}^{\mathrm{i_{b0}}} = \boldsymbol{C}_{\mathrm{b}}^{\mathrm{i_{b0}}}\left(\omega_{\mathrm{ib}}^{\mathrm{b}}\times\right) \tag{22}$$

$$\begin{aligned} \dot{\widehat{\boldsymbol{C}}}_{\mathrm{b}}^{\mathrm{i_{b0}}} &= \widehat{\boldsymbol{C}}_{\mathrm{b}}^{\mathrm{i_{b0}}}\left(\omega_{\mathrm{ib}}^{\mathrm{b}} + \varepsilon^{\mathrm{b}}\right)\times \\ &= \widehat{\boldsymbol{C}}_{\mathrm{b}}^{\mathrm{i_{b0}}}\left[\left(\omega_{\mathrm{ib}}^{\mathrm{b}}\times\right) + \left(\varepsilon^{\mathrm{b}}\times\right)\right] \end{aligned} \tag{23}$$

The estimate matrix ($\widehat{\boldsymbol{C}}_{\mathrm{b}}^{\mathrm{i_{b0}}}$), consisting of the true value ($\boldsymbol{C}_{\mathrm{b}}^{\mathrm{i_{b0}}}$) and error matrix ($\delta\boldsymbol{C}_{b}^{\mathrm{i_{b0}}}$), is given by:

$$\widehat{\boldsymbol{C}}_b^{i_{b0}} = \boldsymbol{C}_b^{i_{b0}} + \delta\boldsymbol{C}_b^{i_{b0}} = \left(\boldsymbol{I} - \phi_2^{i_{b0}}\times\right)\boldsymbol{C}_b^{i_{b0}} \tag{24}$$

Differentiate both sides of the above formula, the equation (25) can be obtained.

$$\dot{\widehat{\boldsymbol{C}}}_b^{i_{b0}} = \left(-\dot{\phi}_2^{i_{b0}}\times\right)\boldsymbol{C}_b^{i_{b0}} + \left(\boldsymbol{I} - \phi_2^{i_{b0}}\times\right)\dot{\boldsymbol{C}}_b^{i_{b0}} \tag{25}$$

Substitute the equation (23) and (24) into the equation (25), the formula is given by:

$$\left(\boldsymbol{I} - \phi_2^{\mathrm{i_{b0}}}\times\right)\boldsymbol{C}_{\mathrm{b}}^{\mathrm{i_{b0}}}\left(\varepsilon^{\mathrm{b}}\times\right) = \left(-\dot{\phi}_2^{\mathrm{i_{b0}}}\times\right)\boldsymbol{C}_{\mathrm{b}}^{\mathrm{i_{b0}}} \tag{26}$$

Known from the above equation (26), the differential equation of misalignment angle matrix ($\dot{\boldsymbol{\phi}}_2^{\mathrm{i_{b0}}}$) can be obtain as:

$$\dot{\phi}_2^{\mathrm{i_{b0}}} = -\boldsymbol{C}_{\mathrm{b}}^{\mathrm{i_{b0}}}\boldsymbol{\varepsilon}^{\mathrm{b}} \tag{27}$$

Integrate the above equation (26), the misalignment angle matrix ($\phi_2^{\mathrm{n}}(t)$) is given by:

$$\begin{aligned} \phi_2^{\mathrm{n}}(t) &= \boldsymbol{C}_{\mathrm{i_{n0}}}^{\mathrm{n}}(t)\boldsymbol{C}_{\mathrm{i_{b0}}}^{\mathrm{i_{n0}}}\phi_2^{\mathrm{i_{b0}}} = -\boldsymbol{C}_{\mathrm{i_{n0}}}^{\mathrm{n}}(t)\int_0^t \boldsymbol{C}_{\mathrm{b}}^{\mathrm{i_{b0}}}(\tau)\boldsymbol{\varepsilon}^{\mathrm{b}}\mathrm{d}\tau \\ &= -\boldsymbol{C}_{\mathrm{i_{n0}}}^{\mathrm{n}}(t)\int_0^t \boldsymbol{C}_{\mathrm{n}}^{\mathrm{i_{n0}}}(\tau)\boldsymbol{\varepsilon}^{\mathrm{n}}\mathrm{d}\tau \end{aligned} \tag{28}$$

For the static-base initial alignment, the attitude of carrier is constant, that is$\boldsymbol{\varepsilon}^{\mathrm{n}} = \boldsymbol{C}_{\mathrm{b}}^{\mathrm{n}}\boldsymbol{\varepsilon}^{\mathrm{b}}$. Substitute the equation (29) (matrix $\boldsymbol{C}_{\mathrm{n}}^{\mathrm{i_{n0}}}$) into the equation (28) and simplified, the equation (30) can be obtained.

$$\begin{aligned} \boldsymbol{C}_{\mathrm{n}}^{\mathrm{i_{n0}}} &= \boldsymbol{I} + \frac{\sin(\omega_{\mathrm{ie}}t)}{\omega_{\mathrm{ie}}}(\omega_{\mathrm{ie}}^{\mathrm{n}}\times) + \frac{1-\cos(\omega_{\mathrm{ie}}t)}{\omega_{\mathrm{ie}}^2}(\omega_{\mathrm{ie}}^{\mathrm{n}}\times)^2 \\ &= \begin{bmatrix} \cos(\omega_{\mathrm{ie}}t) & -\sin L\sin(\omega_{\mathrm{ie}}t) & \cos L\sin(\omega_{\mathrm{ie}}t) \\ \sin L\sin(\omega_{\mathrm{ie}}t) & \cos^2 L + \cos(\omega_{\mathrm{ie}}t)\sin^2 L & [1-\cos(\omega_{\mathrm{ie}}t)]\sin L\cos L \\ -\cos L\sin(\omega_{\mathrm{ie}}t) & [1-\cos(\omega_{\mathrm{ie}}t)]\sin L\cos L & \sin^2 L + \cos(\omega_{\mathrm{ie}}t)\cos^2 L \end{bmatrix} \end{aligned} \tag{29}$$

$$\boldsymbol{\phi}_2^{\mathrm{n}}(t) = \frac{1}{\omega_{\mathrm{ie}}}\begin{bmatrix} -\sin(\omega_{\mathrm{ie}}t) & -\sin L + \cos(\omega_{\mathrm{ie}}t)\sin L & \cos L - \cos(\omega_{\mathrm{ie}}t)\cos L \\ -\sin L\cos(\omega_{\mathrm{ie}}t) + \sin L & -\sin^2 L\sin(\omega_{\mathrm{ie}}t) - \omega_{\mathrm{ie}}t\cos^2 L & \sin L\cos L[\sin(\omega_{\mathrm{ie}}t) - \omega_{\mathrm{ie}}t] \\ \cos L\cos(\omega_{\mathrm{ie}}t) - \cos L & \sin L\cos L[\sin(\omega_{\mathrm{ie}}t) - \omega_{\mathrm{ie}}t] & -\cos^2 L\sin(\omega_{\mathrm{ie}}t) - \omega_{\mathrm{ie}}t\sin^2 L \end{bmatrix}\boldsymbol{\varepsilon}^{\mathrm{n}} \tag{30}$$

For the initial alignment time (t) is typically about two to five minutes, the rotate angle of Earth ($\omega_{ie}t$) is small amount, hence,$\sin(\omega_{ie}t)\approx\omega_{ie}t$,$\cos(\omega_{ie}t)\approx1$. The equation (30) can be simplified as (31).

$$\boldsymbol{\phi}_2^{n}(t)\approx\frac{1}{\omega_{ie}}\begin{bmatrix}-\omega_{ie}t & 0 & 0\\ 0 & -\omega_{ie}t & 0\\ 0 & 0 & -\omega_{ie}t\end{bmatrix}\boldsymbol{\varepsilon}^{n}=-\boldsymbol{\varepsilon}^{n}t \tag{31}$$

2) misalignment angle ϕ_1^{n} analysis.

It is indicated from Section B. Chapter III that the transformation matrix ($\boldsymbol{C}_{i_{b0}}^{i_{n0}}$) can be calculated by equation (7) without the measurement and gravity error. Considering the influence of DOV and IMU errors, the calculation value of matrix ($\widetilde{\boldsymbol{C}}_{i_{b0}}^{i_{n0}}$) is introduced by:

$$\widetilde{C}_{i_{b0}}^{i_{n0}}=C_{i_{b0}}^{i_{n0}}+\delta C_{i_{b0}}^{i_{n0}}=\widetilde{M}_{i_{n0}}^{-T}\widetilde{M}_{i_{b0}}^{T} \tag{32}$$

where the vector matrixes under the inertial navigation frame (i_{n0}) and body frame (i_{b0}) are respectively as follows:

$$\begin{cases}\widetilde{M}_{i_{n0}}^{-T}=M_{i_{n0}}^{-T}+\delta M_{i_{n0}}^{-T}\\ \widetilde{M}_{i_{b0}}^{T}=M_{i_{b0}}^{T}+\delta M_{i_{b0}}^{T}\end{cases} \tag{33}$$

Therefore, the equation (32) can be rewritten as:

$$\begin{aligned}\widetilde{C}_{i_{b0}}^{i_{n0}}&=C_{i_{b0}}^{i_{n0}}+\delta C_{i_{b0}}^{i_{n0}}=C_{i_{b0}}^{i_{n0}}+\left(\phi_1^{i_{n0}}\times\right)C_{i_{b0}}^{i_{n0}}\\ &=\widetilde{M}_{i_{n0}}^{-T}\widetilde{M}_{i_{b0}}^{T}\\ &=\left(M_{i_{n0}}+\delta M_{i_{n0}}\right)^{-T}\left(M_{i_{b0}}+\delta M_{i_{b0}}\right)^{T}\end{aligned} \tag{34}$$

At the same time considering the DOV and IMU errors, the second-order small amount of the coupling is ignored. The error matrix ($\delta C_{i_{b0}}^{i_{n0}}$) can be divided into two components, the attitude transformation error matrix ($\delta C_{i_{b0}}^{i_{n0}}1$) influenced by DOV and the error matrix ($\delta C_{i_{b0}}^{i_{n0}}2$) introduce by IMU errors, shown as equation (35).

$$\delta C_{i_{b0}}^{i_{n0}}=\delta C_{i_{b0}}^{i_{n0}}1+\delta C_{i_{b0}}^{i_{n0}}2=\delta M_{i_{n0}}M_{i_{b0}}^{-1}+M_{i_{n0}}^{-T}\delta M_{i_{b0}}^{T} \tag{35}$$

Compared the above equation and equation (16), the misalignment angle matrix ($\phi_1^{i_{n0}}$) is given by:

$$\begin{aligned}\left(\phi_1^{i_{n0}}\times\right)&=\left(\delta M_{i_{n0}}M_{i_{b0}}^{-1}+M_{i_{n0}}^{-T}\delta M_{i_{b0}}^{T}\right)C_{i_{n0}}^{i_{b0}}\\ &=\delta M_{i_{n0}}M_{i_{b0}}^{-1}C_{i_{n0}}^{i_{b0}}+M_{i_{n0}}^{-T}\delta M_{i_{b0}}^{T}C_{i_{n0}}^{i_{b0}}=M+N\end{aligned} \tag{36}$$

Consequently, the error matrix ($\phi_1^{i_{n0}}$) can also be divided into two components, the alignment errors caused by DOV and IMU errors, to analyze.

(1) $M=\delta M_{i_{n0}}M_{i_{b0}}^{-1}C_{i_{n0}}^{i_{b0}}$ *calculation.*

The vector matrix consisting of gravity vector in two different moments (t_1) and (t_2) under the i_{n0} frame can be described as:

$$\widetilde{M}_{i_{n0}}=\begin{bmatrix}\dfrac{[\widetilde{g}^{i_{n0}}(t_1)]^T}{\|\widetilde{g}^{i_{n0}}(t_1)\|}\\ \dfrac{[\widetilde{g}^{i_{n0}}(t_1)\times\widetilde{g}^{i_{n0}}(t_2)]^T}{\|\widetilde{g}^{i_{n0}}(t_1)\times\widetilde{g}^{i_{n0}}(t_2)\|}\\ \dfrac{[\widetilde{g}^{i_{n0}}(t_1)\times\widetilde{g}^{i_{n0}}(t_2)\times\widetilde{g}^{i_{n0}}(t_1)]^T}{\|\widetilde{g}^{i_{n0}}(t_1)\times\widetilde{g}^{i_{n0}}(t_2)\times\widetilde{g}^{i_{n0}}(t_1)\|}\end{bmatrix}=M_{i_{n0}}+\delta M_{i_{n0}} \tag{37}$$

where the matrixes involved in the above equation can be described as following equations (38)–(41). The vectors $\widetilde{\boldsymbol{g}}^{i_{n0}}(t_1)$ and $\widetilde{\boldsymbol{g}}^{i_{n0}}(t_2)$ denote the projection of gravity vectors in different two moments under the inertial navigation frame (i_{n0}) respectively.

$$\begin{aligned}\frac{\widetilde{g}^{i_{n0}}(t_1)}{\|\widetilde{g}^{i_{n0}}(t_1)\|}&=\frac{g^{i_{n0}}+\delta g^{i_{n0}}}{g}\left(1+\frac{2g^{i_{n0}}\cdot\delta g^{i_{n0}}+\delta g^{i_{n0}}\cdot\delta g^{i_{n0}}}{g^2}\right)^{-\frac{1}{2}}\\ &\approx\frac{g^{i_{n0}}(t_1)}{g}+\frac{\delta g^{i_{n0}}(t_1)}{g}-\frac{g^{i_{n0}}(t_1)\cdot\delta g^{i_{n0}}(t_1)}{g^3}g^{i_{n0}}(t_1)\end{aligned} \tag{38}$$

where $\delta g^{i_{n0}}(t)$ means the error of vector ($\boldsymbol{g}^{i_{n0}}(t)$), which can be given by the multiplying between the DCM and gravity vector$\boldsymbol{g}^{i_{n0}}(t)=C_n^{i_{n0}}(t)\boldsymbol{g}^{n}$,$\delta g^{i_{n0}}(t)=C_n^{i_{n0}}(t)\delta g^{n}$, g denotes the modulo of$\boldsymbol{g}^{i_{n0}}(t)$,$g=\left\|\boldsymbol{g}^{i_{n0}}(t_1)\right\|=g\sqrt{1+(t_1\omega_{ie}\cos L)^2}$.

$$\frac{\widetilde{g}^{i_{n0}}(t_1)\times\widetilde{g}^{i_{n0}}(t_2)}{\|\widetilde{g}^{i_{n0}}(t_1)\times\widetilde{g}^{i_{n0}}(t_2)\|}\approx\frac{r^{i_{n0}}}{r}+\frac{\delta r^{i_{n0}}}{r}-\frac{r^{i_{n0}}\cdot\delta r^{i_{n0}}}{r^3}r^{i_{n0}} \tag{39}$$

where the vectors involved in above equation (39), $\boldsymbol{r}^{i_{n0}}$ and $\delta\mathbf{r}^{i_{n0}}$ are given by equation (40). r means the modulo of$\boldsymbol{r}^{i_{n0}}$.

$$\begin{cases}r^{i_{n0}}=g^{i_{n0}}(t_1)\times g^{i_{n0}}(t_2)\\ \delta r^{i_{n0}}=\delta g^{i_{n0}}(t_1)\times g^{i_{n0}}(t_2)+g^{i_{n0}}(t_1)\times\delta g^{i_{n0}}(t_2)\\ r=\|r\|=g^2\omega_{ie}(t_2-t_1)\cos L\end{cases} \tag{40}$$

$$\frac{\widetilde{g}^{i_{n0}}(t_1)\times\widetilde{g}^{i_{n0}}(t_2)\times\widetilde{g}^{i_{n0}}(t_1)}{\|\widetilde{g}^{i_{n0}}(t_1)\times\widetilde{g}^{i_{n0}}(t_2)\times\widetilde{g}^{i_{n0}}(t_1)\|}=\frac{s^{i_{n0}}}{s}+\frac{\delta s^{i_{n0}}}{s}-\frac{s^{i_{n0}}\cdot\delta s^{i_{n0}}}{s^3}s^{i_{n0}} \tag{41}$$

where the vectors involved in equation (41) are given by (42).

$$\begin{cases}s^{i_{n0}}=g^{i_{n0}}(t_1)\times g^{i_{n0}}(t_2)\times g^{i_{n0}}(t_1)\\ \delta s^{i_{n0}}=\delta g^{i_{n0}}(t_1)\times g^{i_{n0}}(t_2)\times g^{i_{n0}}(t_1)+g^{i_{n0}}(t_1)\times\delta g^{i_{n0}}(t_2)\times g^{i_{n0}}(t_1)\\ \quad+g^{i_{n0}}(t_1)\times g^{i_{n0}}(t_2)\times\delta g^{i_{n0}}(t_1)\\ s=\|s\|=g^3\omega_{ie}\cos L(t_2-t_1)\sqrt{(1+t_1^2\omega_{ie}^2\cos^2 L)}\end{cases} \tag{42}$$

Substitute the equations (38)–(42) into the equation (37), the vector matrix ($\delta M_{i_{n0}}$) can be given by equation (43).

$$\delta M_{i_{n0}} = \begin{bmatrix} \left(\frac{\delta g^{i_{n0}}}{g} - \frac{(g^{i_{n0}}\cdot\delta g^{i_{n0}})g^{i_{n0}}}{g^3}\right)^T \\ \left(\frac{\delta r^{i_{n0}}}{r} - \frac{(r^{i_{n0}}\cdot\delta r^{i_{n0}})r^{i_{n0}}}{r^3}\right)^T \\ \left(\frac{\delta s^{i_{n0}}}{s} - \frac{(s^{i_{n0}}\cdot\delta s^{i_{n0}})s^{i_{n0}}}{s^3}\right)^T \end{bmatrix} = \begin{bmatrix} \frac{(\eta - t_1\omega_{ie}^U\xi)^3 + \xi(t_1\omega_{ie})^3\cos^2 L\sin L}{\left[1+\left(t_1\omega_{ie}^N\right)^2\right]^{\frac{3}{2}}} & \frac{\eta t_1\omega_{ie}^U + \xi}{\sqrt{1+\left(t_1\omega_{ie}^N\right)^2}} & \frac{-\left(\eta t_1\omega_{ie}^N\right)^3 + \xi(t_1\omega_{ie})^2\cos L\sin L}{\left[1+\left(t_1\omega_{ie}^N\right)^2\right]^{\frac{3}{2}}} \\ \eta\tan L & 0 & \xi \\ \frac{-\left(\xi\tan L + \eta t_1\omega_{ie}^N\right)^3 + \xi\tan L\left[1+\left(t_1\omega_{ie}^N\right)^2\right]}{\left[1+\left(t_1\omega_{ie}^N\right)^2\right]^{\frac{3}{2}}} & \frac{-\xi t_1\omega_{ie}^N + \eta\tan L}{\sqrt{1+\left(t_1\omega_{ie}^N\right)^2}} & \frac{\left(-\eta + \xi t_1\omega_{ie}^U\right)^3 - \xi t_1\omega_{ie}^U\left[1+\left(t_1\omega_{ie}^N\right)^2\right]}{\left[1+\left(t_1\omega_{ie}^N\right)^2\right]^{\frac{3}{2}}} \end{bmatrix} \tag{43}$$

$$M_{i_{n0}}^{-T} = \begin{bmatrix} \frac{[g^{i_{n0}}(t_1)]^T}{\|g^{i_{n0}}(t_1)\|} \\ \frac{[g^{i_{n0}}(t_1)\times g^{i_{n0}}(t_2)]^T}{\|g^{i_{n0}}(t_1)\times g^{i_{n0}}(t_2)\|} \\ \frac{[g^{i_{n0}}(t_1)\times g^{i_{n0}}(t_2)\times g^{i_{n0}}(t_1)]^T}{\|g^{i_{n0}}(t_1)\times g^{i_{n0}}(t_2)\times g^{i_{n0}}(t_1)\|} \end{bmatrix}^{-1} = \begin{bmatrix} \left(\frac{g^{i_{n0}}}{g}\right)^T \\ \left(\frac{r^{i_{n0}}}{r}\right)^T \\ \left(\frac{s^{i_{n0}}}{s}\right)^T \end{bmatrix}^{-1} = \begin{bmatrix} -\frac{t_1\omega_{ie}\cos L}{\sqrt{1+(t_1\omega_{ie}\cos L)^2}} & 0 & -\frac{1}{\sqrt{1+(t_1\omega_{ie}\cos L)^2}} \\ 0 & 1 & 0 \\ -\frac{1}{\sqrt{1+(t_1\omega_{ie}\cos L)^2}} & 0 & \frac{t_1\omega_{ie}\cos L}{\sqrt{1+(t_1\omega_{ie}\cos L)^2}} \end{bmatrix} \tag{44}$$

where ω_{ie}^N and ω_{ie}^U are the northward and upward projections of rotation angular rate of Earth under navigation frame (n) respectively.$\omega_{ie}^N = \omega_{ie}\cos L$,$\omega_{ie}^U = \omega_{ie}\sin L$.

It can be indicated from equation (36) that, the calculation of misalignment angle ($\phi_1^{i_{n0}}$) consists of the right side of the equation. For the convenience to calculate matrix (***M***), transpose the first term of the right side of equation (36), which is given by equation (45).

$$M^T = C_{i_{b0}}^{i_{n0}} M_{i_{b0}}^{-T}\delta M_{i_{n0}}^T = M_{i_{n0}}^{-T}\delta M_{i_{n0}}^T \tag{45}$$

Substitute the equation (43) and (44) into (45) ignoring the second-order values, the matrix (***M***) can be simplified as:

$$M^T = \begin{bmatrix} 0 & \eta\tan L & -\eta \\ -\eta\tan L & 0 & \xi \\ \eta & -\xi & 0 \end{bmatrix} \tag{46}$$

(2) $N = M_{i_{n0}}^{-T}\delta M_{i_{b0}}^T C_{i_{n0}}^{i_{b0}}$ calculation.

In the last section, the misalignment angular error caused by DOV has been analyzed, while the error influenced by IMU measurement errors is introduced in this section.

Known from the second term of the right side in equation (36), the matrix (***N***) can be calculated by matrixes ($\boldsymbol{M}_{i_{n0}}^{-T}$) given by equation (44) and ($\delta M_{i_{b0}}^T$) determined by formula (47).

$$\widetilde{\boldsymbol{M}}_{i_{b0}}^{T} = \begin{bmatrix} \frac{\left[\widetilde{\boldsymbol{g}}^{i_{b0}}(t_1)\right]^T}{\left\|\widetilde{\boldsymbol{g}}^{i_{b0}}(t_1)\right\|} \\ \frac{\left[\widetilde{\boldsymbol{g}}^{i_{b0}}(t_1)\times\widetilde{\boldsymbol{g}}^{i_{b0}}(t_2)\right]^T}{\left\|\widetilde{\boldsymbol{g}}^{i_{b0}}(t_1)\times\widetilde{\boldsymbol{g}}^{i_{b0}}(t_2)\right\|} \\ \frac{\left[\widetilde{\boldsymbol{g}}^{i_{b0}}(t_1)\times\widetilde{\boldsymbol{g}}^{i_{b0}}(t_2)\times\widetilde{\boldsymbol{g}}^{i_{b0}}(t_1)\right]^T}{\left\|\widetilde{\boldsymbol{g}}^{i_{b0}}(t_1)\times\widetilde{\boldsymbol{g}}^{i_{b0}}(t_2)\times\widetilde{\boldsymbol{g}}^{i_{b0}}(t_1)\right\|} \end{bmatrix} \tag{47}$$

where the gravity vector projection under inertial body frame (i_{b0}) can be calculated by equation (21).

Considering the constant zero bias errors of accelerometers and ignoring the second-order amounts, the equation (21) can be rewritten as:

$$\begin{aligned} \widetilde{g}^{i_{b0}}(t) &= g^{i_{b0}}(t) + \delta g^{i_{b0}}(t) = -\widehat{C}_b^{i_{b0}}(t)\widetilde{f}^b(t) \\ &= -\left[I - \phi_2^{i_{b0}}(t)\times\right]C_b^{i_{b0}}(t)\left(-g^b + \nabla^b\right) \\ &\approx g^{i_{b0}}(t) - \nabla^{i_{b0}}(t) - \phi_2^{i_{b0}}(t)\times g^{i_{b0}}(t) \\ &= C_{i_{n0}}^{i_{b0}}C_n^{i_{n0}}(t)\left[g^n - \nabla^n - \phi_2^n(t)\times g^n\right] \end{aligned} \tag{48}$$

Known from the equation (48), the gravity vector error $\delta\mathbf{g}^{i_{b0}}(t)$ can be given by:

$$\begin{aligned} \delta g^{i_{b0}}(t) &= C_{i_{n0}}^{i_{b0}}C_n^{i_{n0}}(t)\left[-\nabla^n - \phi_2^n(t)\times g^n\right] \\ &= C_n^{i_{n0}}(t)\left[-\nabla^n - \phi_2^n(t)\times g^n\right]C_{i_{b0}}^{i_{n0}} \end{aligned} \tag{49}$$

Similar with the equations (38)–(42), the vectors in inertial body frame can be given as:

$$\frac{\widetilde{g}^{i_{b0}}(t_1)}{\left\|\widetilde{g}^{i_{b0}}(t_1)\right\|} = \frac{g^{i_{b0}}(t_1)}{g} + \frac{\delta g^{i_{b0}}(t_1)}{g} - \frac{g^{i_{b0}}(t_1)\cdot\delta g^{i_{b0}}(t_1)}{g^3}g^{i_{b0}}(t_1) \tag{50}$$

$$\frac{\widetilde{g}^{i_{b0}}(t_1)\times\widetilde{g}^{i_{b0}}(t_2)}{\left\|\widetilde{g}^{i_{b0}}(t_1)\times\widetilde{g}^{i_{b0}}(t_2)\right\|} = \frac{p^{i_{b0}}}{p} + \frac{\delta p^{i_{b0}}}{p} - \frac{p^{i_{b0}}\cdot\delta p^{i_{b0}}}{p^3}p^{i_{b0}} \tag{51}$$

$$\frac{\widetilde{g}^{i_{b0}}(t_1)\times\widetilde{g}^{i_{b0}}(t_2)\times\widetilde{g}^{i_{b0}}(t_1)}{\left\|\widetilde{g}^{i_{b0}}(t_1)\times\widetilde{g}^{i_{b0}}(t_2)\times\widetilde{g}^{i_{b0}}(t_1)\right\|} = \frac{q^{i_{b0}}}{q} + \frac{\delta q^{i_{b0}}}{q} - \frac{q^{i_{b0}}\cdot\delta q^{i_{b0}}}{q^3}q^{i_{b0}} \tag{52}$$

where the vectors involved in the above equations are given by:

$$\begin{cases} p^{i_{b0}} = g^{i_{b0}}(t_1)\times g^{i_{b0}}(t_2) \\ \delta p^{i_{b0}} = \delta g^{i_{b0}}(t_1)\times g^{i_{b0}}(t_2) + g^{i_{b0}}(t_1)\times\delta g^{i_{b0}}(t_2) \\ p = \|p\| = g^2\omega_{ie}(t_2 - t_1)\cos L \end{cases} \tag{53}$$

$$\begin{cases} q^{i_{b0}} = g^{i_{b0}}(t_1)\times g^{i_{b0}}(t_2)\times g^{i_{b0}}(t_1) \\ \delta q^{i_{b0}} = \delta g^{i_{b0}}(t_1)\times g^{i_{b0}}(t_2)\times g^{i_{b0}}(t_1) + g^{i_{b0}}(t_1)\times\delta g^{i_{b0}}(t_2)\times g^{i_{b0}}(t_1) \\ \quad + g^{i_{b0}}(t_1)\times g^{i_{b0}}(t_2)\times\delta g^{i_{b0}}(t_1) \\ q = \|q\| = g^3\omega_{ie}(t_2 - t_1)\cos L \end{cases} \tag{54}$$

According to the relationship of coordinate transformation, the vector ($\boldsymbol{g}^{i_{b0}}(t)$) can be given by:

$$g^{i_{b0}}(t) = C_{i_{n0}}^{i_{b0}}C_n^{i_{n0}}(t)g^n \tag{55}$$

Substitute the equations (48)–(55) into the equation (47) and ignore the second-order amount, the matrix ($\delta M_{i_{b0}}^T$) is given as equation (56) and the matrix (***N***) can be rewritten as equation (57).

$$\delta M_{i_{b0}}^{T}=\begin{bmatrix}\left(\frac{\delta g^{i_{b0}}}{g}-\frac{(g^{i_{b0}}\cdot\delta g^{i_{b0}})g^{i_{b0}}}{g^{3}}\right)^{T}\\ \left(\frac{\delta p^{i_{b0}}}{p}-\frac{(p^{i_{b0}}\cdot\delta p^{i_{b0}})p^{i_{b0}}}{p^{3}}\right)^{T}\\ \left(\frac{\delta q^{i_{b0}}}{q}-\frac{(q^{i_{b0}}\cdot\delta q^{i_{b0}})q^{i_{b0}}}{q^{3}}\right)^{T}\end{bmatrix}=\begin{bmatrix}\left[\left(I+t_1\omega_{ie}^{n}\times\right)(\varepsilon^{n}t_1\times g^{n}-\nabla^{n})\right]^{T}\\ \left\{\begin{matrix}\left[\left(I+t_1\omega_{ie}^{n}\times\right)(\varepsilon^{n}t_1\times g^{n}-\nabla^{n})\right]\times\left[\left(I+t_2\omega_{ie}^{n}\times\right)g^{n}\right]+\\ \left[\left(I+t_1\omega_{ie}^{n}\times\right)g^{n}\right]\times\left[\left(I+t_2\omega_{ie}^{n}\times\right)(\varepsilon^{n}t_2\times g^{n}-\nabla^{n})\right]\end{matrix}\right\}^{T}\\ \left\{\begin{matrix}\left[\left(I+t_1\omega_{ie}^{n}\times\right)(\varepsilon^{n}t_1\times g^{n}-\nabla^{n})\right]\times\left[\left(I+t_2\omega_{ie}^{n}\times\right)g^{n}\right]\times\left[\left(I+t_1\omega_{ie}^{n}\times\right)g^{n}\right]+\\ \left[\left(I+t_1\omega_{ie}^{n}\times\right)g^{n}\right]\times\left[\left(I+t_2\omega_{ie}^{n}\times\right)(\varepsilon^{n}t_2\times g^{n}-\nabla^{n})\right]\times\left[\left(I+t_1\omega_{ie}^{n}\times\right)g^{n}\right]+\\ \left[\left(I+t_1\omega_{ie}^{n}\times\right)g^{n}\right]\times\left[\left(I+t_2\omega_{ie}^{n}\times\right)g^{n}\right]\times\left[\left(I+t_1\omega_{ie}^{n}\times\right)(\varepsilon^{n}t_1\times g^{n}-\nabla^{n})\right]\end{matrix}\right\}^{T}\end{bmatrix}C_{i_{b0}}^{i_{n0}} \tag{56}$$

$$N=M_{i_{n0}}^{-T}\delta M_{i_{b0}}^{T}C_{i_{n0}}^{i_{b0}}=M_{i_{n0}}^{-T}\begin{bmatrix}\left[\left(I+t_1\omega_{ie}^{n}\times\right)(\varepsilon^{n}t_1\times g^{n}-\nabla^{n})\right]^{T}\\ \left\{\begin{matrix}\left[\left(I+t_1\omega_{ie}^{n}\times\right)(\varepsilon^{n}t_1\times g^{n}-\nabla^{n})\right]\times\left[\left(I+t_2\omega_{ie}^{n}\times\right)g^{n}\right]+\\ \left[\left(I+t_1\omega_{ie}^{n}\times\right)g^{n}\right]\times\left[\left(I+t_2\omega_{ie}^{n}\times\right)(\varepsilon^{n}t_2\times g^{n}-\nabla^{n})\right]\end{matrix}\right\}^{T}\\ \left\{\begin{matrix}\left[\left(I+t_1\omega_{ie}^{n}\times\right)(\varepsilon^{n}t_1\times g^{n}-\nabla^{n})\right]\times\left[\left(I+t_2\omega_{ie}^{n}\times\right)g^{n}\right]\times\left[\left(I+t_1\omega_{ie}^{n}\times\right)g^{n}\right]+\\ \left[\left(I+t_1\omega_{ie}^{n}\times\right)g^{n}\right]\times\left[\left(I+t_2\omega_{ie}^{n}\times\right)(\varepsilon^{n}t_2\times g^{n}-\nabla^{n})\right]\times\left[\left(I+t_1\omega_{ie}^{n}\times\right)g^{n}\right]+\\ \left[\left(I+t_1\omega_{ie}^{n}\times\right)g^{n}\right]\times\left[\left(I+t_2\omega_{ie}^{n}\times\right)g^{n}\right]\times\left[\left(I+t_1\omega_{ie}^{n}\times\right)(\varepsilon^{n}t_1\times g^{n}-\nabla^{n})\right]\end{matrix}\right\}^{T}\end{bmatrix}a+ \tag{57}$$

Subsequently, the equation (44) is substituted into the matrix (***N***) reserving the first-order values with ignoring the error term about $\boldsymbol{\varepsilon t}$ as well as high-order amounts. Simplified the equation (57) and the matrix (***N***) can be ultimately given by:

$$N=\begin{bmatrix}0 & \frac{1}{g}\nabla_E\tan L-\frac{1}{\omega_{ie}^{N}}\varepsilon_E & \frac{1}{g}\nabla_E\\ \frac{1}{g}\nabla_E\tan L-\frac{1}{\omega_{ie}^{N}}\varepsilon_E & 0 & -\frac{1}{g}\nabla_N\\ \frac{1}{g}\nabla_E & -\frac{1}{g}\nabla_N & 0\end{bmatrix} \tag{58}$$

And then, substitute the equation (46) and (58) into the formula (36), the misalignment angle caused by DOV and IMU errors ($\boldsymbol{\phi}_1^{i_{n0}}$) can be obtained as equation (59).

$$\phi_1^{i_{n0}}=\begin{bmatrix}-\frac{\nabla_N}{g}-\xi & \frac{\nabla_E}{g}+\eta & \left(\frac{\nabla_E}{g}+\eta\right)\tan L-\frac{1}{\omega_{ie}^{N}}\varepsilon_E\end{bmatrix}^{T} \tag{59}$$

$$\phi^{n}=\phi_1^{n}+\phi_2^{n}=C_{i_{n0}}^{n}\phi_1^{i_{n0}}+\phi_2^{n}\approx\begin{bmatrix}-\frac{\nabla_N}{g}-\xi\\ \frac{\nabla_E}{g}+\eta\\ \left(\frac{\nabla_E}{g}+\eta\right)\tan L-\frac{1}{\omega_{ie}^{N}}\varepsilon_E\end{bmatrix} \tag{60}$$

Ultimately, the equations (31) and (59) are substituted into the equation (20), the misalignment angle, caused by the coupling of DOV and IMU errors, of initial alignment is introduced as equation (60).

It is indicated from equation (60) that the DOV components are coupled with the errors of horizontal inertial sensors reflected in the misalignment angles. The values of DOV directly restrain the alignment accuracy. In the respect of eastward and northward components of misalignment angle, the DOV components can be precisely estimated by horizontal misalignment angle, if the zero bias of horizontal accelerometers can be effectively suppressed. Based on the previous analysis, a novel DOV calculation method, estimated by misalignment angles based on single-axis rotating modulation is proposed and specifically introduced in the next chapter.

5. DOV Estimation Method and Kalman Filter

5.1. The principle of single-axis rotating modulation error suppression

Relative to the single-position alignment, the single-axis rotation modulation method continuously rotates the IMU relative to the carrier around the azimuth axis at a constant angular rate, which not only makes the system completely observe but also the constant error of horizontal IMU can be modulated into a periodic signal which integrated to zero in a fixed rotation period, to suppress the constant error of the horizontal inertial sensors to the initial alignment.

The constant drift bias errors and zero bias errors of gyroscopes and accelerometers are supposed to express as (ε_x), (ε_y), (ε_z) and (∇_x), (∇_y), (∇_z) respectively. For the initial moment, the IMU frame (s) is consistent with the body frame (b) and the IMU rotates around the azimuth axis at a constant angular rate (ω). Consequently, the transformation relation between the IMU frame and body frame can be expressed as equation (61) and the errors of IMU under body frame after rotation can be determined by equations (62) and (63) respectively.

$$\boldsymbol{C}_{\mathrm{s}}^{\mathrm{b}}=\begin{bmatrix}\cos\omega t & -\sin\omega t & 0\\ \sin\omega t & \cos\omega t & 0\\ 0 & 0 & 1\end{bmatrix} \tag{61}$$

$$\begin{bmatrix}\varepsilon_{\mathrm{x}}^{\mathrm{b}}\\ \varepsilon_{\mathrm{y}}^{\mathrm{b}}\\ \varepsilon_{\mathrm{z}}^{\mathrm{b}}\end{bmatrix}=\begin{bmatrix}\varepsilon_{\mathrm{x}}\cos\omega t-\varepsilon_{\mathrm{y}}\sin\omega t\\ \varepsilon_{\mathrm{x}}\sin\omega t+\varepsilon_{\mathrm{y}}\cos\omega t\\ \varepsilon_{\mathrm{y}}\end{bmatrix} \tag{62}$$

$$\begin{bmatrix}\nabla_{\mathrm{x}}^{\mathrm{b}}\\ \nabla_{\mathrm{y}}^{\mathrm{b}}\\ \nabla_{\mathrm{z}}^{\mathrm{b}}\end{bmatrix}=\begin{bmatrix}\nabla_{\mathrm{x}}\cos\omega t-\nabla_{\mathrm{y}}\sin\omega t\\ \nabla_{\mathrm{x}}\sin\omega t+\nabla_{\mathrm{y}}\cos\omega t\\ \nabla_{\mathrm{y}}\end{bmatrix} \tag{63}$$

Known from equations (62) and (63), the constant errors of the horizontal inertial sensors become the periodic signals after being modulated by single-axis rotation, and the integral of the signals is zero

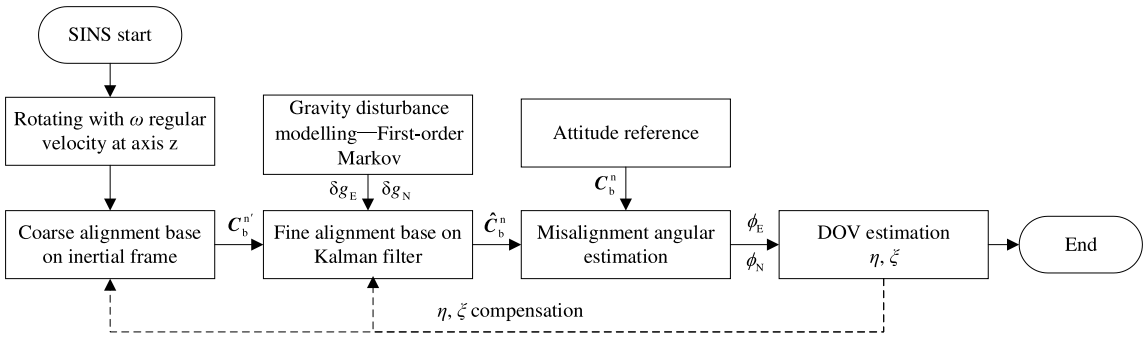

Fig. 3. Process of DOV estimation.

within one complete rotation period. It is indicated from equation (60) that the initial alignment error is mainly related to constant errors of horizontal inertial sensors. Hence, the rotation modulation can effectively suppress the horizontal inertial sensors errors and the constant errors of sensors during a rotation period is introduced as the following paper.

There is a constant drift in the laser gyroscope and zero bias in the accelerometers, which affect the horizontal and azimuth alignment accuracy in the initial alignment of SINS. Integrate the equations (62) and (63) during a rotation period, which can be given by:

$$\begin{aligned}\nabla_{\mathrm{E}} &= \frac{\int_0^t \left(\nabla_x \cos\omega t - \nabla_y \sin\omega t\right)\mathrm{d}\tau}{t} = \frac{\int_0^t \sqrt{\nabla_x^2+\nabla_y^2}\cos(\omega t+\alpha)\mathrm{d}\tau}{t} \\ &= \frac{\sqrt{\nabla_x^2+\nabla_y^2}}{\omega t}\left[\sin(\omega t+\alpha)-\sin\alpha\right]\end{aligned} \tag{64}$$

$$\alpha = \arccos\frac{\nabla_x}{\sqrt{\nabla_x^2+\nabla_y^2}}$$

Same as equation (64), the northward zero bias and eastward drift can be calculated by:

$$\begin{aligned}\nabla_{\mathrm{N}} &= \frac{\int_0^t \left(\nabla_x \sin\omega t + \nabla_y \cos\omega t\right)\mathrm{d}\tau}{t} = \frac{\int_0^t \sqrt{\nabla_x^2+\nabla_y^2}\sin(\omega t+\alpha)\mathrm{d}\tau}{t} \\ &= -\frac{\sqrt{\nabla_x^2+\nabla_y^2}}{\omega t}\left[\cos(\omega t+\alpha)-\cos\alpha\right]\end{aligned} \tag{65}$$

$$\begin{aligned}\varepsilon_{\mathrm{E}} &= \frac{\int_0^t \left(\varepsilon_x \cos\omega t - \varepsilon_y \sin\omega t\right)\mathrm{d}\tau}{t} = \frac{\int_0^t \sqrt{\varepsilon_x^2+\varepsilon_y^2}\cos(\omega t+\beta)\mathrm{d}\tau}{t} \\ &= \frac{\sqrt{\varepsilon_x^2+\varepsilon_y^2}}{\omega t}\left[\sin(\omega t+\beta)-\sin\beta\right]\end{aligned} \tag{66}$$

$$\beta = \arccos\frac{\varepsilon_x}{\sqrt{\varepsilon_x^2+\varepsilon_y^2}}$$

The horizontal and azimuth alignment errors caused by constant drift and zero bias of gyroscopes and accelerometers are given by equations (67)-(69) respectively.

$$\phi_{\mathrm{E}} = -\frac{\nabla_{\mathrm{N}}}{g} = -\frac{\sqrt{\nabla_x^2+\nabla_y^2}}{g\omega t}\left[\cos(\omega t+\alpha)-\cos\alpha\right] \tag{67}$$

$$\phi_{\mathrm{N}} = \frac{\nabla_{\mathrm{E}}}{g} = -\frac{\sqrt{\nabla_x^2+\nabla_y^2}}{g\omega t}\left[\sin(\omega t+\alpha)-\sin\alpha\right] \tag{68}$$

It can be seen from equations (67)–(69) that the horizontal and azimuth misalignment angle has been modulated into the periodic signals after the rotating modulation. Besides, the horizontal misalignment angle is related to the zero bias of horizontal accelerometers (∇_x,∇_y), rotation angular rate of the turntable (ω) and the alignment time (t). At the same time, the integration of the horizontal misalignment angle caused by IMU errors during a rotation period is zero, which means the misalignment angles after rotating modulation directly reflect the DOV information on static-base. Consequently, based on the previous analysis, the specific process of the DOV estimation method is introduced in Section C.

$$\begin{aligned}\phi_{\mathrm{U}} &= \frac{\nabla_{\mathrm{E}}}{g}\tan L - \frac{\varepsilon_{\mathrm{E}}}{\omega_{\mathrm{ie}}\cos L} \\ &= -\frac{\tan L\sqrt{\nabla_x^2+\nabla_y^2}}{g\omega t}\left[\sin(\omega t+\alpha)-\sin\alpha\right] - \frac{\sqrt{\varepsilon_x^2+\varepsilon_y^2}}{\omega_{\mathrm{ie}}\cos L\omega t}\left[\sin(\omega t+\beta)\right. \\ &\quad \left.-\sin\beta\right]\end{aligned} \tag{69}$$

5.2. Kalman filter model based on DOV modeling.

Kalman filter, a classical optimal estimation theory, widely applicated for state estimation in linear systems. For the initial alignment of SINS, the adaptive condition of Kalman filter is under the small misalignment angle. Consequently, the process of initial alignment is generally divided into two procedures, coarse alignment of inertial frame and fine alignment based on Kalman filter.

According to the error equations of SINS, the attitude and velocity error equations of single-axis rotating laser SINS on static-base can be expressed as:

$$\dot{\phi}^n = -\omega_{ie}^n \times \phi^n - C_b^n C_p^b \varepsilon^p \tag{70}$$

$$\delta\dot{v}^n = f^n \times \phi^n + C_b^n C_p^b \nabla^p + \delta g^n \tag{71}$$

where matrix (ϕ^{n}) means the misalignment angles, ε^p and ∇^{p} denote the constant drift and zero bias of gyroscopes and accelerometers under the IMU frame (p) respectively.

From section A chapter IV analysis, it can be known that the DOV components initially have an impact on the velocity error and then affect the attitude error. Consequently, it is necessary to construct the gravity disturbance model to satisfy with Kalman filter equations under the dynamic measured situation and not required modeled under static base or waggling base.

Under the dynamic measured situation, the gravity disturbance model of the whole trajectory can be modeled as the first-order Markov model, where the autocorrelation and the power spectral densities functions of the first-order Markov model are introduced by:

$$\begin{cases} C_x(\tau) = \sigma^2 e^{-\zeta|\tau|} \\ \Phi_x(\omega) = \dfrac{2\sigma^2\zeta}{\omega^2+\zeta^2} \end{cases} \tag{72}$$

Table 1
Simulation Parameters setup.

Conditions	Parameters	Accuracy
IMU	Gyro. Constant drift ε^{b}	0.01°/h
	Gyro. Random walk ε^{b}	0.001°/$h^{1/2}$
	Acce. Constant zero bias ∇^{b}	100 μg
	Acce. Random walk ∇^{b}	10 μg/$Hz^{1/2}$
Alignment time	Total time	6 min
	Coarse alignment time	3 min
	Fine alignment time	5 min
Rotating condition	Rotating angle	3600°
	Rotating time	5 min
DOV	East-west η	5″
	South-north ξ	18″

where σ means the mean square variance of gravity disturbance and ζ is the reciprocal of time.

The state and discretization equations of gravity disturbance can be written as:

$$\delta\dot{g}(t) = -\zeta\delta g(t) + \sqrt{2\zeta\sigma^2}w(t) \tag{73}$$

$$\delta g_k = e^{-\zeta\Delta t}\delta g_{k-1} + \sigma\sqrt{1-e^{-2\zeta\Delta t}}w_{k-1} \tag{74}$$

The system state equation and observation equation in Kalman filter are given by:

$$\begin{cases} \dot{X} = FX + GW \\ Z = HX + V \end{cases} \tag{75}$$

where $X = [\phi^n \quad \delta V^n \quad \varepsilon^p \quad \nabla^p \quad \delta g^n]^T$ is the system state vector, including misalignment, velocity error, gyroscope drift, accelerometer zero bias, and horizontal gravity disturbance. The matrixes $\boldsymbol{F}$ and $\boldsymbol{G}$ are state transform matrix and distribution matrix of system noise respectively, which are shown as:

$$F = \begin{bmatrix} (-\omega_{ie}^n\times)_{3\times3} & 0_{3\times3} & -C_b^nC_{p_{3\times3}}^b & 0_{3\times3} & 0_{3\times3} \\ (f^n\times)_{3\times3} & 0_{3\times3} & 0_{3\times3} & C_b^nC_{p_{3\times3}}^b & I_{3\times3} \\ & & 0_{3\times15} & & \\ & & 0_{3\times15} & & \\ & & 0_{3\times12} & F_{1_{3\times3}} & \end{bmatrix} F_1$$

$$= \begin{bmatrix} -\zeta_1 & 0 & 0 \\ 0 & -\zeta_2 & 0 \\ 0 & 0 & -\zeta_3 \end{bmatrix}, \quad G = \begin{bmatrix} -C_b^n & 0_{3\times3} & 0_{3\times3} \\ 0_{3\times3} & C_b^n & 0_{3\times3} \\ 0_{6\times3} & 0_{6\times3} & 0_{6\times3} \\ 0_{3\times3} & 0_{3\times3} & I_{3\times3} \end{bmatrix}, \quad W = \begin{bmatrix} w_g^b \\ w_a^b \\ w_{dg}^n \end{bmatrix}$$

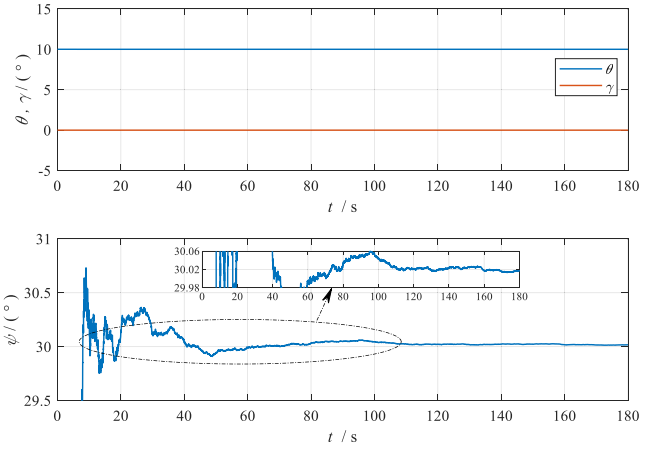

Fig. 4. Attitude angles without rotation.

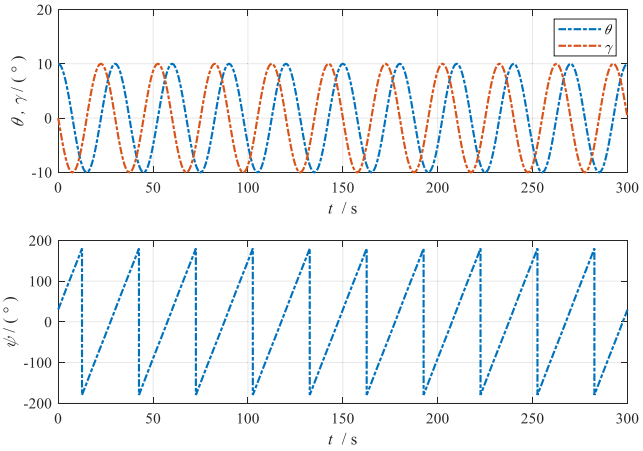

Fig. 5. Attitude angles with rotation.

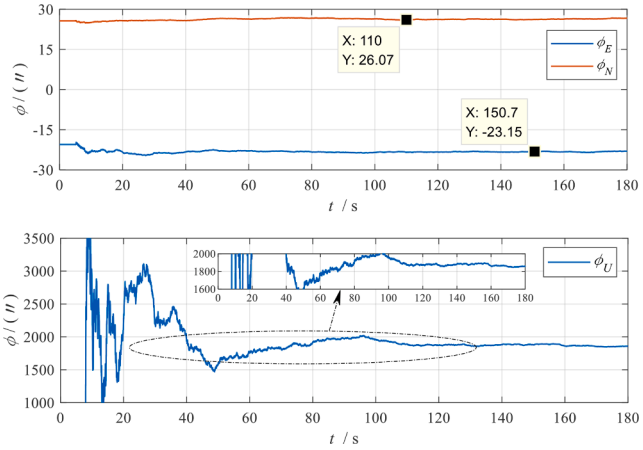

Fig. 6. Misalignment angles in coarse alignment without rotation.

$\boldsymbol{W}$ is the system noise, which can be considered as zero-mean random white noise. $\boldsymbol{Z}$ denotes the observation state, as for the zero-speed theory of static-base initial alignment, the output of SINS ($\boldsymbol{V}^n$) is velocity error ($\delta\boldsymbol{V}^n$) and acceleration error can be calculated by the differential of velocity, ignoring upward channel, which is given by:$\boldsymbol{Z} = [\boldsymbol{V}_E^n \quad \boldsymbol{V}_N^n]^T$.

$\boldsymbol{H}$ denotes the observation matrix defined as:

$$H = [0_{2\times3} \quad I_{2\times2} \quad 0_{2\times10}]$$

$\boldsymbol{V}$ is the measurement noise that assumed to be white noise.

5.3. DOV estimation process on static base

From the analysis in the previous sections, it can be indicated that the DOV components can be estimated from the horizontal misalignment angles by rotating modulation. For the static-base of SINS, the inertial frame coarse alignment combined with the fine alignment based on Kalman filter with single-axis rotating method is proposed to estimate the DOV components from misalignment angle of initial alignment. The specific process of this method is shown as Fig. 3.

It is obvious from Fig. 3. that the coarse alignment provides attitude transformation matrix ($\boldsymbol{C}_b^{n'}$) for fine alignment based on Kalman filter. Subsequently, the difference between the attitude estimation matrix ($\widehat{\boldsymbol{C}}_b^n$) and reference attitude ($\boldsymbol{C}_b^n$) is used to obtain the estimated value of the misalignment angle. Eventually, the DOV components (ξ, η) are estimated by horizontal misalignment angle (ϕ_E, ϕ_N) respectively. In addition, the dotted arrow line in Fig. 3 indicates the DOV compensation process for initial alignment, which will improve the performance of

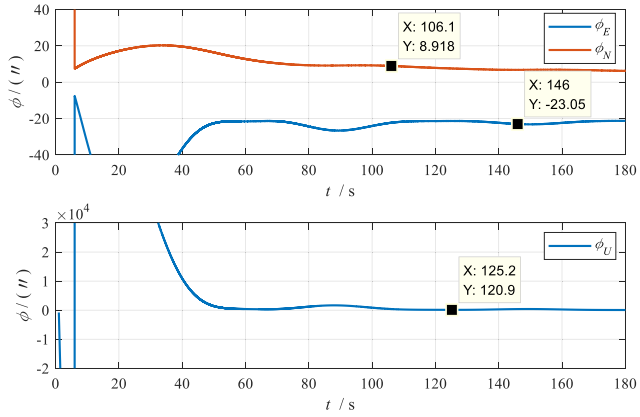

Fig. 7. Misalignment angles in coarse alignment with rotation.

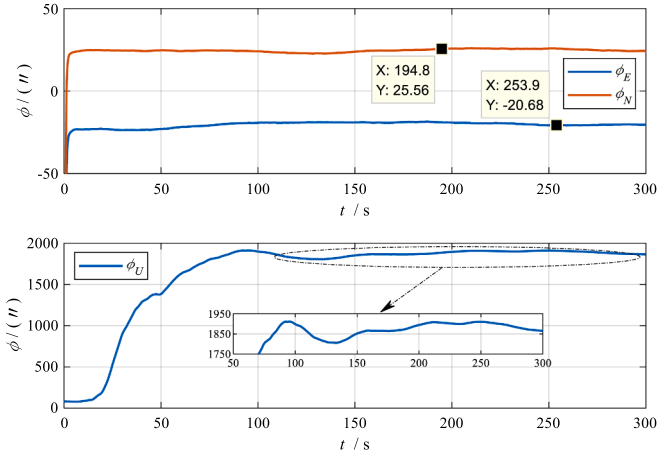

Fig. 8. Misalignment angles in fine alignment without rotation.

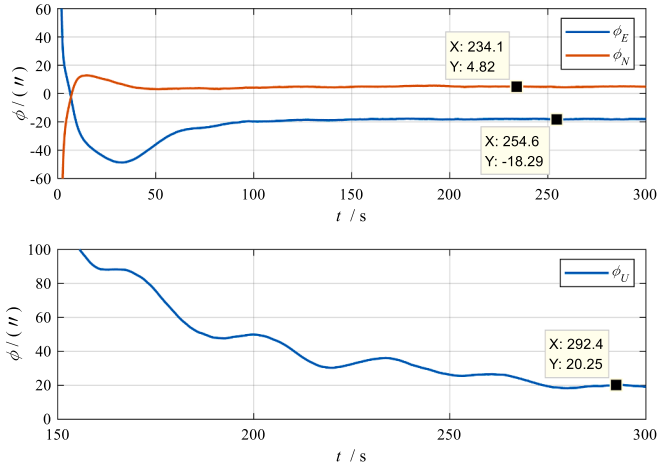

Fig. 9. Misalignment angles in fine alignment with rotation.

alignment accuracy.

6. Simulations

To verify the validity of theoretical analysis for error derivation of initial alignment in chapter IV and the performance of the DOV estimation method based on single-axis rotating modulation, the experiments on initial alignment with and without rotating modulation were conducted and specifically introduced in this chapter.

Table 2
Experiments Results.

	DOV estimation value		DOV true value	
	$\hat{\eta}/('')$	$\hat{\xi}/('')$	$\eta/('')$	$\xi/('')$
1	4.73	18.03	5.00	18.00
2	5.14	18.07		
3	5.53	16.62		
4	5.85	17.91		
5	5.01	17.99		
6	5.03	18.26		
7	4.85	17.31		
8	4.74	17.67		
9	5.18	17.55		
10	5.05	17.91		
Mean value	5.111	17.732		
RMSE	0.349	0.479		

6.1. Simulation conditions setup

The simulation conditions, listed in Table 1, were set as follows: The latitude and longitude were N-34°1′48″ and E-108°45′52″ respectively. The carrier speed is set as zero and the initial attitude angles, the pitch (θ), roll (γ) and heading angle (ψ) were 10°, 0°, 30° respectively. From the perspective of IMU, the constant drift and random drift biases of gyroscopes were set as 0.01°/h and 0.001°/$h^{1/2}$, while the constant zero bias and random walk coefficient of accelerometers were 100 μg and 10 μg/$Hz^{1/2}$. The time of total alignment was set as 6 min, the coarse alignment base on the inertial frame was 3 min, while the fine alignment based on Kalman filter was 5 min, where the first two minutes data reutilized the last 2 min data of coarse alignment. When under the rotating modulation conditions, the rotating time was 5 min and the total rotating angle was 3600°. The IMU data were generated after the addition of DOV components which were set as 5″ and 18″ respectively.

6.2. Analysis of DOV estimation results

The results of attitude angles with and without rotation are shown in Fig. 4 and Fig. 5 respectively. As can be seen from the figures, the horizontal attitude angles (θ, γ) rapidly converge to the theoretical values and the heading angle was gradually convergence to fluctuate around the theoretical value without the rotation. While in the rotating modulation condition, the horizontal attitudes are modulated as the sinusoidal signal and the heading angle became the sawtooth signal.

The misalignment angles in coarse alignment with and without

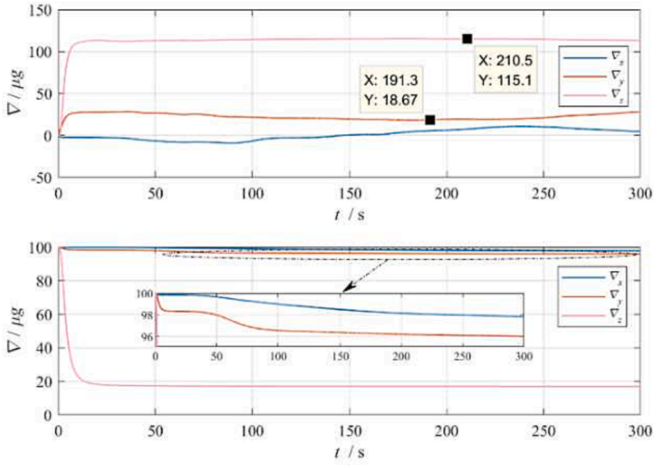

Fig. 10. Estimation of accelerometers without rotation.

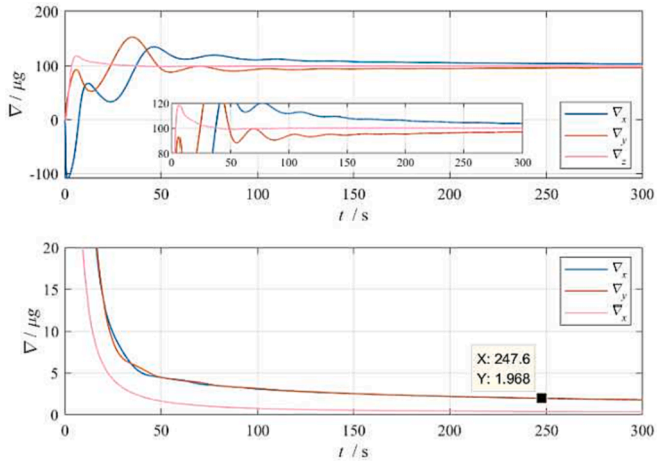

Fig. 11. Estimation of accelerometers with rotation.

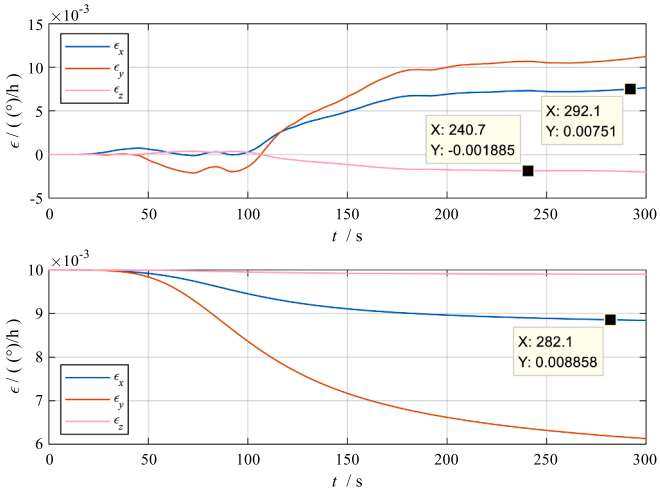

Fig. 12. Estimation of gyroscopes without rotation.

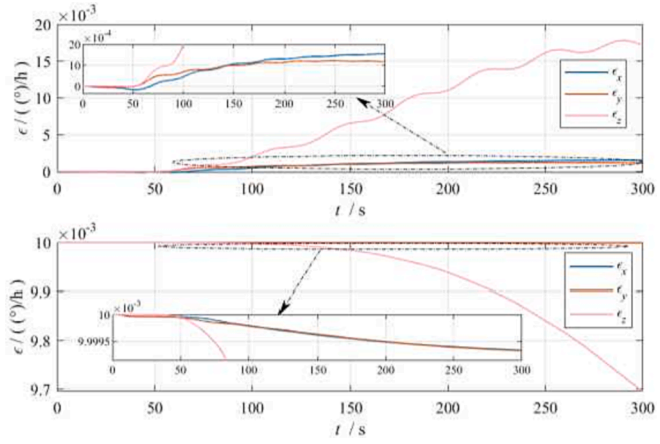

Fig. 13. Estimation of gyroscopes with rotation.

rotation are plotted in Fig. 6 and Fig. 7, while the fine alignment results under two conditions are shown in Fig. 8 and Fig. 9 respectively. It can be seen from the figures that the misalignment angles are significantly reduced with rotating modulation both in coarse alignment and fine alignment, particularly in upward misalignment angles. This is mainly because the horizontal errors of inertial sensors are effectively suppressed by rotating modulation, which is consistent with the theoretical analysis in chapter V.

It is indicated from the horizontal misalignment angles in Figs. 6-9 that the DOV components are coupled with accelerometer errors, under the condition without rotation, while in the coarse alignment with rotating modulation, the horizontal misalignment angles are converged nearby the true values. However, the estimation results in coarse alignment with rotation still cannot effectively suppress the accelerometers errors. While in the fine alignment with rotating modulation, the horizontal misalignment angles are extremely converged to the DOV true values, which can be effectively estimated as DOV components based on formula (60), shown in Fig. 9.

The results of DOV values estimated by horizontal misalignment angles selected from experiments are listed in Table 2. It can be known from the table that the estimation of DOV components from horizontal misalignment angles are extremely closed to the theoretical true values of DOV. The root means square (RMS) results of the DOV components (η, ξ) are 0.349″ and 0.479″ respectively. Consequently, the estimation results of DOV validated the correctness of previous theoretical analysis in chapter IV/V and are consistent with the equation (60) and (67)–(68). The performance of the proposed method can satisfy the requirements for the accuracy of DOV.

6.3. Estimation of inertial sensor errors

In this section, the errors estimation analysis of the inertial sensors based on the Kalman filter with and without rotation is performed. The accelerometer constant zero biases are plotted in Fig. 10 and Fig. 11 in two conditions, while the gyroscope constant drift biases are plotted in Fig. 12 and Fig. 13. It is obvious from Fig. 10 and Fig. 11 that the constant zero biases hardly be effectively estimated without rotation. In this respect, this is mainly because the observabilities of accelerometer zero biases are too low and cannot be effectively estimated by Kalman filter. On the contrary, while in the rotation condition, the accelerometer zero biases can be more accurately estimated from state value in the Kalman filter, shown as Fig. 11.

From the perspective of the gyroscope, the drift biases estimation of three-axis basically reach convergence after the 150 s. However, as for the limitation of observabilities, the convergence results are inconsistent with true values. When in the rotation condition, the drift biases of x/y-axis accelerometers effectively converge to the true values, while the z-axis accelerometer cannot converge because of the rotation around the z-axis.

Consequently, after the rotating modulation, the observability of inertial sensors errors has been improved and the fine alignment based on Kalman filter can effectively estimate the inertial sensors constant errors from the state values.

6.4. Influence of Dov and gravity anomaly on alignment attitude angle error

To further analyze the influence of DOV and gravity anomaly on alignment attitude angle error, the six different cases of dual-position alignment experiments were conducted. The five cases of DOV and gravity anomaly are listed in Table 3, and the IMU parameters are shown

Table 3
Parameters setup.

	DOV		Gravity Anomaly
	η/(″)	ξ/(″)	Δg/(mGal)
Case1	5	−10	0
Case2	10	−10	0
Case3	5	−20	0
Case4	5	−10	50
Case 5	0	0	0

Table 4
Parameters setup.

Conditions	Parameters	Accuracy
IMU	Sample rate	100 Hz
	Gyro. Constant drift ε^b	0.005°/h
	Gyro. Random walk ε^b	0.0005°/h$^{1/2}$
	Acce. Constant zero bias ∇^b	50 μg
	Acce. Random walk ∇^b	5 μg/Hz$^{1/2}$
Inertial alignment	Algorithm samples	4
	Attitude updating time	0.04 s

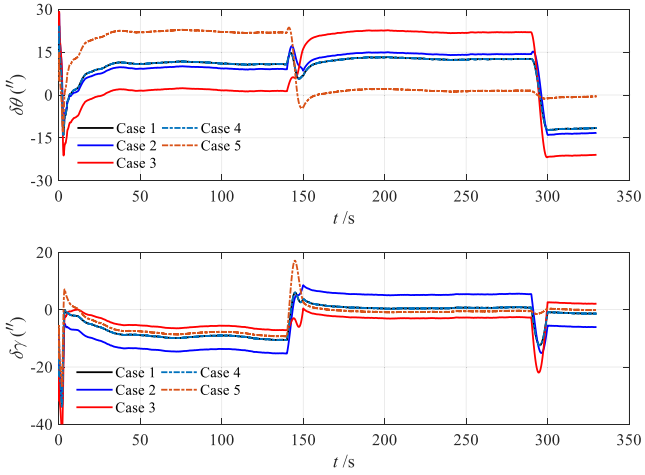

Fig. 14. Pitch and roll angle errors of six cases.

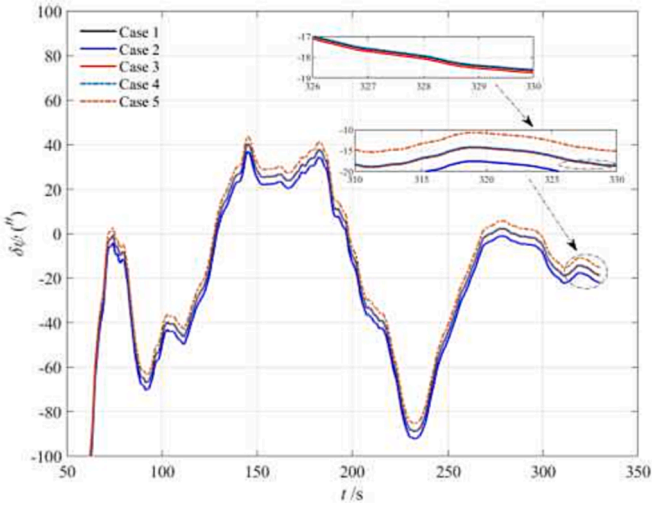

Fig. 15. Heading angle errors of six cases.

Table 5
GDV and DOV parameters.

	δg_E /(mGal)	Δg_N /(mGal)
	η/('')	ξ/('')
GDV	46.58	−121.74
DOV	−9.81	25.64

in Table 4. The total time during the alignment is 5 min. During the first 140 s, the IMU is static in the first position and then rotated 180° to the second position in 10 s, subsequently, the IMU is similarly static in the second position for 140 s and rotated 180° back to the first position

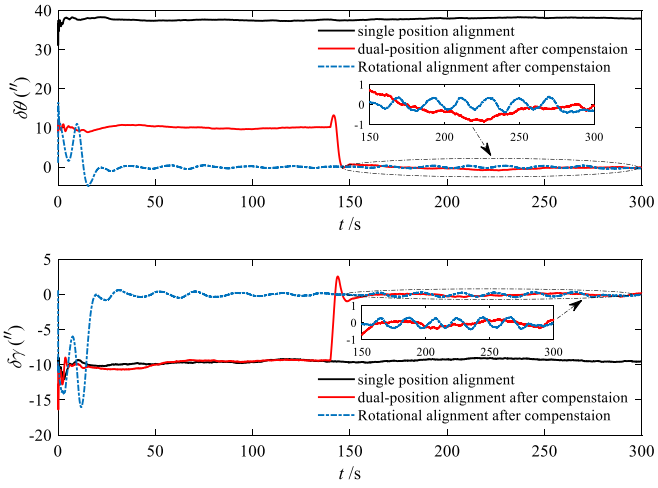

Fig. 16. Pitch and roll angle errors.

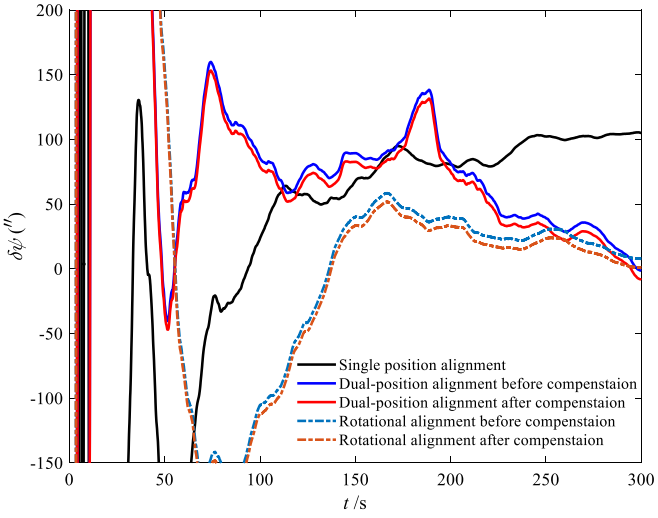

Fig. 17. Heading angle errors.

(a) Double-axis SINS (b) Pendulous scope

Fig. 18. Alignment experiment equipment system.

during within 10 s. In order to clearly reflect the convergence, the 30 s was added in the last position. Consequently, the total time was set as 330 s under this condition.

The simulation results of pitch, roll, and heading angle errors are shown in Figs. 14 and 15 respectively. It can be obviously observed that the orange dotted line (Case 5) is converged around the zero with rotational modulation, which is consistent with the parameters of case 5.

The misalignment angles (ϕ_E, ϕ_N, ϕ_U) are conventionally converted into the attitude angle errors ($\delta\theta$, $\delta\gamma$, $\delta\psi$) for analysis and the transformation equation can be known from [25]. Consequently, the theoretical values of the attitude angle errors can be obtained by substituting equation (60) into the transformation equation, and the simulation results in the figures are all converged to the corresponding theoretical values of five cases.

Comparing the case 1 and case 2, it can be known that the pitch angle errors are almost consistent, while the roll angle error of case 2 is greater about 5′′ than case 1, which is consistent with the incremental parameters between the case 1 and 2 (η) of the Table 3. In addition, the compared results of the Case 1 and 3 demonstrate the incremental of south-to-north component (ξ). Moreover, the results of case 1 and case 4 indicate that the gravity anomaly has no effect on alignment attitude angle error. Consequently, it can be concluded that the south-to-north component (ξ) and east-to-west component (η) directly affect the values of pitch angle error and roll angle error, while the heading angle error is commonly affected by (ξ) and (η).

7. Experiments

7.1. Simulation of DOV compensation on alignment

In order to directly reflect the influence of DOV and the promotion of accuracy after compensation on the attitude angle error of initial alignment based on rotational modulation, this section is mainly introduced the effects of DOV compensation on dual-position alignment and continuous-rotation alignment. The IMU parameters are same set as the previous section, the latitude and longitude are N 34°1′48′′ E 108°45′52′′ respectively. The GDV as well as the DOV, calculated by EIGEN-6c4 gravity field model, are listed in Table 5.

The horizontal attitude angle errors and heading angle error are shown in Figs. 16 and 17 respectively. It can be indicated that the attitude angle errors of single position alignment before DOV compensation are more obvious because of the couple influence of accelerometers errors and DOV, while the errors of dual-position alignment and continuous-rotation alignment are all almost reduced to around the zero with DOV compensation.

7.2. Experiments of DOV compensation on alignment

The rotational modulation experiments of dual-positions and continuous-rotation were conducted and the accuracy increasement of alignment after DOV compensation is mainly analyzed in this section.

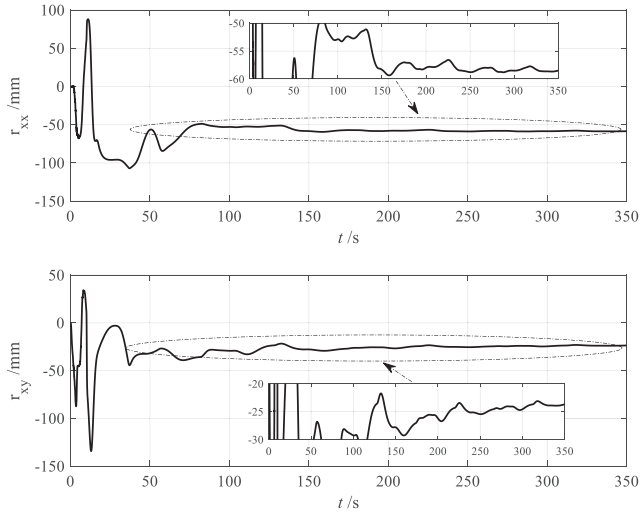

Fig. 19. Size effect estimation of x-axis.

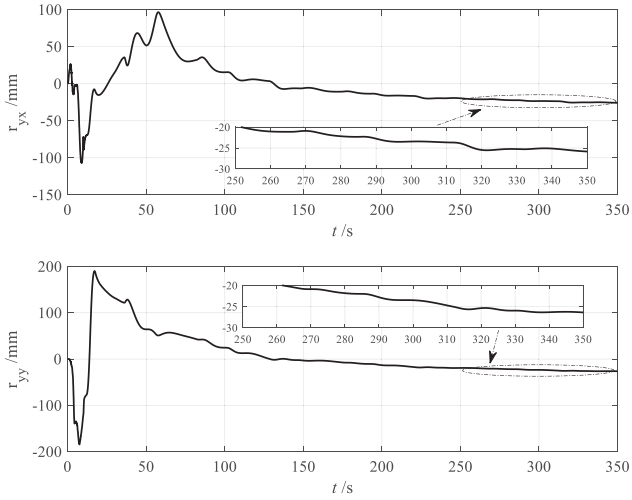

Fig. 20. Size effect estimation of y-axis.

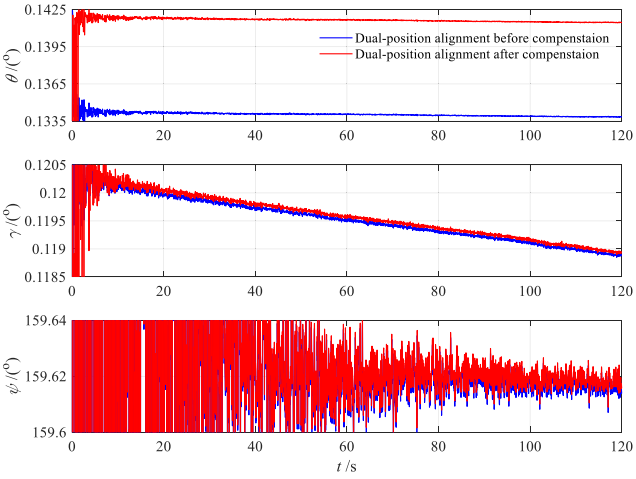

Fig. 21. The attitude angles before and after compensation.

Table 6
Experiments Results.

	Before compensation /(′)	After compensation /(′)	True value /(′)
1	9576.574	9576.684	9577.379
2	9576.467	9576.573	
3	9576.738	9576.826	
4	9576.589	9576.681	
5	9576.932	9577.106	
6	9576.745	9576.836	
7	9577.174	9577.277	
8	9576.914	9577.124	
9	9576.425	9576.538	
10	9577.029	9577.132	
Mean value	9576.759	9576.878	
RMSE	0.696	0.591	

The theoretical true value of heading angle was 9577.379′, which can be precisely measured by pendulous gyroscope, shown as Fig. 18.

In the experiment, coarse alignments were set for 120 s and fine alignment using Kalman filtering for 240 s. The IMU sampling interval is 0.01 s; After the self-calibration experiment of SINS, the laser gyroscope constant drifts are 0.0050, 0.0048, and 0.0045°/h respectively, and the

corresponding random walk coefficients were 0.00046, 0.00044, and 0.00047°/$h^{1/2}$ respectively, while the accelerometer constant zero biases were 47, 51, 37 μg, respectively.

The size effect estimations of horizontal accelerometers are shown in Figs. 19 and 20. Moreover, the constant drifts, install angle errors and scale factor error of IMU as well as the size effect of accelerometers caused by rotation have been eliminated in data process. Fig. 21 indicates the variation of attitude angles with and without DOV compensation of coarse alignment based on dual-positions alignment, and the ten groups of final alignment results of continues rotation are listed in Table 6.

To evaluate the promotion in heading angle performance after compensation, the RMSE of experiments was calculated for the heading angle before and after compensation. It is indicated that the RMSE of the heading angle before and after DOV compensation are 0.696' and 0.591′ respectively. The error is reduced about 6′'.

8. Conclusion

From the perspective of the inertial navigation field, the plumb plane and normal plane are normally mixed in navigation process ignoring the influence of DOV. This will directly cause the horizontal direction errors of gravity vector, thus affecting the alignment and navigation accuracies. With the development of inertial technology, this influence has become one of the main errors in orientation and position. In this respect, the theoretical limit error equation of initial alignment, considering the coupling of IMU errors and DOV, has been specifically derived based on inertial frame alignment theory. It is pointed out that the DOV components straightforward caused the values of horizontal misalignment angles. Based on the results of theoretical analysis, the DOV estimated method, calculated by horizontal misalignment angles with rotating modulation, has been proposed. Finally, the initial alignment experiments with and without rotation are conducted to comparatively analyze the performance of the proposed method. Moreover, the comparative simulations of influences of DOV and gravity anomaly on alignment attitude angle error as well as the DOV compensation simulations and experiments were implemented. It can be concluded that the DOV components directly cause the horizontal attitude angle errors, while the gravity anomaly has no effect.

The simulations results of DOV estimation indicate that the RMSEs of the DOV components of the proposed method are 0.349″ and 0.479″ respectively, which validate the correctness of the theoretical analysis and feasibility of the proposed method. And the experiment results of DOV compensation show that the RMSE of heading angle error is reduced by about 6′'.

CRediT authorship contribution statement

Shiwen Hao: Conceptualization, Methodology, Validation, Writing – original draft. **Zhili Zhang:** Investigation, Resources, Supervision. **Zhaofa Zhou:** Supervision, Funding acquisition. **Zhenjun Chang:** Writing – review & editing. **Zhihao Xu:** Validation. **Xinyu Li:** Data curation.

Declaration of Competing Interest

The authors declare that they have no known competing financial interests or personal relationships that could have appeared to influence the work reported in this paper.

Data availability

The data that has been used is confidential.

Acknowledgment

The authors would like to acknowledge Aviation Science Foundation of China (Grant No. 201808U8004) and Postdoctoral Science Foundation of China (Grant No. 2017 M613372) to provide fund for conducting experiments.

References

[1] N. El-Sheimy, S. Nassar, A. Noureldin, Wavelet de-noising for IMU alignment, IEEE Aerosp. Electron. Syst. Mag. 19 (10) (2004) 32–39.
[2] S. Feng, S. Wei, Mooring alignment for marine SINS using the digital filter, Measurement 43 (10) (2010) 1489–1494.
[3] C. Lubin, J. Shu, et al., Initial Alignment by Attitude Estimation for Strapdown Inertial Navigation Systems, IEEE Trans. Instrum. Meas. 64 (3) (2015) 784–794.
[4] X. Liu, X. Xu, Y. Zhao, et al., An initial alignment method for strapdown gyrocompass based on gravitational apparent motion in inertial frame, Measurement 55 (2014) 593–604.
[5] J. Li, W. Gao, Y.a. Zhang, Z. Wang, Gradient Descent Optimization-Based Self-Alignment Method for Stationary SINS, IEEE Trans. Instrum. Meas. 68 (9) (2019) 3278–3286.
[6] Gl Ea Son D M. Gravity Vector Estimation from Integrated GPS/Strapdown IMU Data[J]. Navigation 39(2) (1992) 237–253.
[7] Q. Li, Y. Ben, F. Sun, A novel algorithm for marine strapdown gyrocompass based on digital filter, Measurement 46 (1) (2013) 563–571.
[8] D. Dai, X. Wang, D. Zhan, et al., Dynamic measurement of high-frequency deflections of the vertical based on the observation of INS/GNSS integration attitude error, J. Appl. Geophys. 119 (2015) 89–98.
[9] Silson, Mg P. Coarse Alignment of a Ship's Strapdown Inertial Attitude Reference System Using Velocity Loci[J]. 60(6) (2011) 1930–1941.
[10] Z. Chuanbin, T. Weifeng, J. Zhihua, A novel method improving the alignment accuracy of a strapdown inertial navigation system on a stationary base, Meas. Sci. Technol. 15 (4) (2004) 765–769.
[11] P.O. Hanson, Correction for deflections of the vertical at the runup site, IEEE Position Location & Navigation Symposium. (1988) 288–296.
[12] C. Jekeli, Precision Free-Inertial Navigation with Gravity Compensation by an Onboard Gradiometer, J. Guid. Control Dynam. 29 (3) (2006) 704–713.
[13] J. Fang, L. Chen, J. Yao, et al., An Accurate Gravity Compensation Method for High-Precision Airborne POS, IEEE Trans. Geosci. Remote Sens. 52 (8) (2014) 4564–4573.
[14] L. Chang, F. Qin, M. Wu, Gravity Disturbance Compensation for Inertial Navigation System, IEEE Trans. Instrum. Meas. 68 (10) (2018) 1–15.
[15] C. Jekeli, J.K. Lee, J.H. Kwon, On the computation and approximation of ultra-high-degree spherical harmonic series, J. Geod. 81 (9) (2007) 603–615.
[16] Z. Zhu, B. Zhao, Y. Guo, et al., Research on gravity vertical deflection on attitude of position and orientation system and compensation method, Aerosp. Sci. Technol. 85 (2) (2019) 495–504.
[17] J. Wang, G. Yang, X. Li, et al., Application of the spherical harmonic gravity model in high precision inertial navigation systems, Meas. Sci. Technol. 27 (9) (2016), 095103.
[18] J. Tie, J. Cao, M. Wu, et al., Compensation of Horizontal Gravity Disturbances for High Precision Inertial Navigation, Sensors 18 (3) (2018) 906–927.
[19] R. Wu, Q. Wu, F. Han, et al., Gravity Compensation Using EGM2008 for High-Precision Long-Term Inertial Navigation Systems, Sensors 16 (12) (2016) 2176–2193.
[20] C. Hirt, B. Buerki, A. Somieski, et al., Modern Determination of Vertical Deflections Using Digital Zenith Cameras, J. Surv. Eng. 136 (1) (2010) 1–12.
[21] D. Dai, X. Wang, D. Zhan, et al., An Improved Method for Dynamic Measurement of Deflections of the Vertical Based on the Maintenance of Attitude Reference, Sensors 14 (2014) 16323–16342.
[22] J. Zhu, Z. Zhou, Y. Li, et al., Further development of the attitude difference method for estimating deflections of the vertical in real time, Meas. Sci. Technol. 27 (2) (2016) 754–768.
[23] H. Xiong, D. Dai, Y. Zhao, et al., An Analysis of the Attitude Estimation Errors Caused by the Deflections of Vertical in the Integration of Rotational INS and GNSS, Sensors 19 (7) (2019) 1721–1738.
[24] W. An, J. Xu, H. He, et al., A Method of Deflection of the Vertical Measurement based on Attitude Difference Compensation, IEEE Sens. J. 99 (7) (2021) 103–111.
[25] Y.Y. Qin, Inertial navigation, Beijing Science Press, 2014.